https://doi.org/10.5194/egusphere-2025-1010
Preprint. Discussion started: 12 March 2025

A helicopter-based mass balance approach for quantifying methane emissions from industrial activities, applied for coal mine ventilation shafts in Poland

Eric Förster[1], Heidi Huntrieser[1], Michael Lichtenstern[1], Falk Pätzold[2], Lutz Bretschneider[2], Andreas Schlerf[2], Sven Bollmann[2], Astrid Lampert[2], Jarosław Nęcki[3], Paweł Jagoda[3], Justyna Swolkień[4], Dominika Pasternak[5,a], Robert A. Field[6] and Anke Roiger[1]

[1]DLR – Deutsches Zentrum für Luft- und Raumfahrt, Institut für Physik der Atmosphäre, Oberpfaffenhofen, Germany
[2]TUBS – Technische Universität Braunschweig, Institute of Flight Guidance, Braunschweig, Germany
[3]AGH – University of Kraków, Faculty of Physics and Applied Computer Science, Kraków, Poland
[4]AGH – University of Kraków, Faculty of Civil Engineering and Recourse Management., Kraków, Poland
[5]Wolfson Atmospheric Chemistry Laboratories, University of York, UK
[6]UNEP's International Methane Emissions Observatory, Paris, France
[a]now at DLR – Deutsches Zentrum für Luft- und Raumfahrt, Flight Experiment, Oberpfaffenhofen, Germany

Correspondence to: Eric Förster (Eric.Foerster@dlr.de) and Heidi Huntrieser (Heidi.Huntrieser@dlr.de)

Status: 03 March 2025

Abstract.

This study introduces a helicopter-borne mass balance approach, utilizing the *HELiPOD* platform, to accurately quantify methane (CH_4) emissions from coal mining activities. Compared to conventional research aircraft the use of an external sling load configuration eliminates the need for aeronautical certifications, facilitates easier modifications and enables local helicopter companies to conduct flights. Furthermore, it allows for plume probing as close as several hundred meters downwind of an emission source and offers comprehensive vertical coverage from 50 m to 3 km altitude, making the *HELiPOD* an ideal tool to distinguish, capture, and quantify emissions from single sources in complex emission landscapes worldwide. Our approach serves as an independent emission verification tool, bridging the gap between ground-based, drone, near-field and far-field airborne measurements and supports identification of CH_4 emission mitigation opportunities. Nineteen mission flights were conducted in the Upper Silesian Coal Basin of Southern Poland in June and October 2022 that targeted CH_4 emissions from multiple coal mine ventilation shafts and several drainage stations. The comparison of top-down *HELiPOD* mass flux estimates against those calculated from bottom-up in-mine CH_4 safety sensor and air flow measurements revealed very good agreement with relative deviations of 0 % to 25 %. This indicates, notwithstanding associated uncertainties, that the two independent approaches are capable of estimating CH_4 emissions from coal mine ventilation shafts. However, the accuracy and representativeness of derived in-mine data is application-specific and should be evaluated by independent measurements. With measured emission rates up to 3,000 kg h^{-1} from individual coal mine ventilation shafts we confirm prior research while revealing that emission strengths from drainage stations can be of comparable magnitude and should be investigated further. The possibility to detect emission rates as low as 20 kg h^{-1} with the *HELiPOD* was demonstrated through a controlled release experiment. This emphasises the wide range of potential applications in quantifying sources within a wide range of CH_4 emission rates, i.e from relatively small sources, e.g. biodigesters, landfills, cattle feedlots and manure pits to larger industrial sources including those from the coal, oil and gas sectors.

https://doi.org/10.5194/egusphere-2025-1010
Preprint. Discussion started: 12 March 2025

1 Introduction

Here we present a helicopter-borne mass balance approach focusing on CH_4 emissions from coal mining activities in Poland. The deployment of the exceptionally versatile measurement platform *HELiPOD* (Pätzold et al., 2023) with state-of-the-art mass balance analysis (Cambaliza et al., 2014; Conley et al., 2017; Heimburger et al., 2017; Hajny et al., 2023) is a new methodological approach for estimating CH_4 fluxes. More recently, this application has been deployed in studies on other anthropogenic sources as from the oil, gas and waste sector (Huntrieser et al., 2023a, b; Förster et al., in preparation for ACP).

The importance of reducing methane (CH_4) emissions to mitigate the future impacts of climate change is well known (Kirschke et al., 2013; Saunois et al., 2020; Forster et al., 2021). The largest mitigation potentials are predicted for the energy and waste sectors. Eliminating venting, reducing flaring and unintended leakages by introducing new technologies, monitoring and repairing of existing equipment are effective within the oil and gas (O&G) sector (Nisbet et al., 2020). Using fugitive CH_4 emissions as an energy source, the oxidation of ventilation air methane (VAM) and pre-mine degasification (gas removal, see e.g. Thakur, 2014) are identified as critical actions for the coal sector (Karacan et al., 2024). Anaerobic digestion with gas recovery and full source separation/recycling of waste have been shown to reduce emissions from waste management. If combined, such efforts could lead to a reduction of the total radiative forcing by 13% until the end of this century (Höglund-Isaksson, 2012; Harmsen et al., 2020; Höglund-Isaksson et al., 2020; Nisbet et al., 2020; Shindell et al., 2024).
International efforts are brought together through the Global Methane Pledge (GMP) (www.globalmethanepledge.org) with the shared goal to reduce global CH_4 emissions by at least 30 % from 2020 levels until 2030. As of January 2025, 159 countries have joined, representing slightly over 50% of all global anthropogenic CH_4 emissions. This figure would rise substantially if coal producing countries, e.g. China, India, Russia and South Africa, sign the GMP, given that the coal sector is estimated to account for approximately a third of the global anthropogenic CH_4 emissions from the energy sector. In 2023, China announced the Methane Emissions Control Action Plan that aims to scientifically and cooperatively manage and control CH_4 emissions (China Ministry of Ecology and Environment, 2023). This act signalling recognition of the importance of mitigation from a country estimated to have the great potential for reduction of CH_4 emissions.

To support mitigation efforts related to the GMP and to track progress over time (UNEP, 2024), the United Nations Environment Programme (UNEP) collects, synthesises and shares actionable CH_4 data through its International Methane Emissions Observatory (IMEO). Through CH_4 science studies, sharing satellite data via the Methane Alert and Response System (MARS), with the Oil and Gas Methane Partnership 2.0 (OGMP 2.0) and from national emission inventory reporting (e.g. through the United Nations Framework Convention on Climate Change, UNFCCC) IMEO supports the production of accurate actionable data to help drive mitigation of emissions. Ground-based, airborne and satellite studies use different measurement strategies to estimate CH_4 mass fluxes (Gorchov Negron et al., 2020; Neininger et al., 2021; Korbeń et al., 2022; Naus et al., 2023; Pühl et al., 2024; UNEP, 2024). The goal of these studies is to reconcile the often discrepant bottom-up (company estimates based on emission factors, inventories and ground-based measurements) and top-down (drone, air- and spaceborne measurements of emissions) estimates and improve the understanding of the uncertainties of different CH_4 source quantification approaches (Höglund-Isaksson, 2017; Vaughn et al., 2018; Kelly et al., 2022; Riddick et al., 2024). With a better knowledge of emission magnitudes and associated uncertainties, more efficient mitigation strategies can be developed.

Satellite imagery has identified the Upper Silesian Coal Basin (USCB) in Southern Poland as a hotspot for atmospheric CH_4 (Schneising et al., 2019; Schuit et al., 2023) where coal mine ventilation shafts are recognised as the major pathway through which CH_4 is emitted to the atmosphere (Swolkień, 2020). These CH_4 point sources are often isolated and a suitable testbed for our application. They have already been investigated in previous measurement studies. Such measurements range from ground-based (e.g. Luther et al., 2019; Dreger and Kędzior, 2021; Menoud et al., 2021) to drone (Andersen et al., 2021, 2023),

https://doi.org/10.5194/egusphere-2025-1010
Preprint. Discussion started: 12 March 2025

airborne (Fiehn et al., 2020; Kostinek et al., 2021) and spaceborne measurements (Krautwurst et al., 2021). Recently, in-mine CH_4 safety sensors were used for the estimation of CH_4 mass fluxes (Swolkień et al., 2022; Nęcki et al., in prep. for AMT). Validation of the application of in-mine safety sensors to estimate ventilation shaft emissions has shown that while specified uncertainties of the safety sensors are high, their measured CH_4 concentrations are in close agreement with high precision instrumentation installed in the shafts (Nęcki et al., in prep. for AMT).

However, up to now there is a gap in the data coverage between ground-based measurements, conducted close to the coal mine facilities at a distance of up to 100 m, the airborne measurements, performed at distances of several km downwind of the source (Fiehn et al., 2020; Kostinek et al., 2021; Luther et al., 2022; Swolkień et al., 2022) and satellite observations, which are at the moment only able to detect sources with emission rates larger 100 kg h^{-1} (Chulakadabba et al., 2023; Naus et al., 2023; Schuit et al., 2023; McLinden et al., 2024). Closing the gap between a distance of ~100 m to 3000 m is important to be able to separate emissions of nearby sources, while covering the entire vertical extension of the single plumes for applying a mass balance approach. This gap can partly be covered by drone measurements (Andersen et al., 2021), notwithstanding limited vertical extent (<120 m in the drone category 'open'), horizontal coverage (maintaining a visual line of sight between operator and drone), flight time (< 20 min), and payload weight (Burgués and Marco, 2020). The latter negating the use of some high quality CH_4 instruments.

Our novel *HELiPOD* set-up efficiently closes this gap, covering the entire distance between *near field* (CH_4 plume impacted by turbulence) and *far field* (CH_4 plume impacted by wind speed/direction and atmospheric stability). As a result, more reliable CH_4 mass flux estimates can be expected. The unique helicopter-borne measurement system *HELiPOD* is equipped with a variety of greenhouse gas, aerosol, meteorological and radiation instruments, see Pätzold et al. (2023) for a detailed technical description. This platform is more flexible than most research aircraft and drones in many aspects:

- Aeronautical certification is not needed for the *HELiPOD*, since it is operated as sling load, only attached mechanically to the helicopter by rope.
- Local helicopter companies can be chosen which negates issues associated with flight permissions while enabling easier implementation of flights due to local knowledge.
- The versatility of the helicopter allows for plume probing much closer to the sources than feasible by small aircraft. This is especially advantageous for separating and quantifying single sources in a complex emission landscape.
- Lower altitudes can be reached with full vertical coverage of the plumes from 50 m up to 3000 m altitude.
- More sophisticated CH_4 instrumentation can be operated on the *HELiPOD* compared to drones, and high-resolution wind measurements can be carried out simultaneously.

Within the UNEP funded METHANE-To-Go-Poland (MTG-Poland) field campaigns, conducted in June and October 2022 in the USCB area, the *HELiPOD* system was deployed for the first time to estimate CH_4 mass fluxes based on the mass balance approach. Four different coal mine ventilation shafts were evaluated, and each shaft was targeted with 2 to 5 flights. In summary, 19 flights were carried out, each with a duration of 2 to 3 hours. An overview of the flights is given in the Supplement S1 in Table S1. The last two flights of the field campaign were dedicated validating our applied methodology by quantifying CH_4 emission rates from a simple controlled release experiment. Finally, our top-down CH_4 mass flux concentrations are compared to bottom-up estimates based on CH_4 safety sensor data from the owners of the coal mines. In this work, we describe the helicopter-borne application for measuring CH_4 emissions close to point sources (Sect. 2) and present the results together with sensitivity studies for reliable CH_4 mass flux calculations, which are further discussed (Sect. 3). We close with a summary and conclusions in Sect. 4.

https://doi.org/10.5194/egusphere-2025-1010
Preprint. Discussion started: 12 March 2025

2 Instrumentation and Methods

In this section, we briefly describe the set-up of the MTG-Poland field experiment in the USCB (Sect. 2.1) and the helicopter-borne platform *HELiPOD* and its instrumentation (Sect. 2.2). In Sect. 2.3 we introduce the well-established mass balance approach for estimating CH_4 mass fluxes and describe our sampling strategy (Sect. 2.4.) with associated uncertainties (Sect. 2.5), supportive ground-based measurements (Sect. 2.6) and CH_4 safety sensor measurements in coal mine ventilation shafts (Sect. 2.7). In Sect. 2.8 we describe the set-up of a controlled CH_4 release experiment.

2.1 Study region

The field experiment was set up in the USCB in Southern Poland and conducted in two separate measurement campaigns from 11–23 June 2022 and from 8–19 October 2022 to cover different the weather conditions anticipated in summer and autumn (see Supplement S1). The campaign base was at the Bielsko-Biała airfield (EPBA, 49° 48.30' N, 19° 0.12' E) south of Katowice at a distance of 25 km to 50 km from the measurement area.

The USCB is known as a hotspot for CH_4 emissions that result from coal mining activities (e.g. Schneising et al., 2019; Tu et al., 2022; Schuit et al., 2023). Figure 1 illustrates the importance of CH_4 emissions in the USCB in the context of Poland for 2022. The targets of the helicopter mission flights were four pre-selected coal mine ventilation shafts with a preference to target metallurgical coal, high CH_4 emissions strengths and mine owners willing to share data. Isolated locations further away from cities and other industries were preferentially selected with a road network that facilitated the mobile ground-based measurements, as described in Sect. 2.6. The probed shafts were Knurow-Szczyglowice IV, Brzeszcze-Andrzej IX, Pniowek V and Agnieszka-Powietrzny V (see Fig. 1).

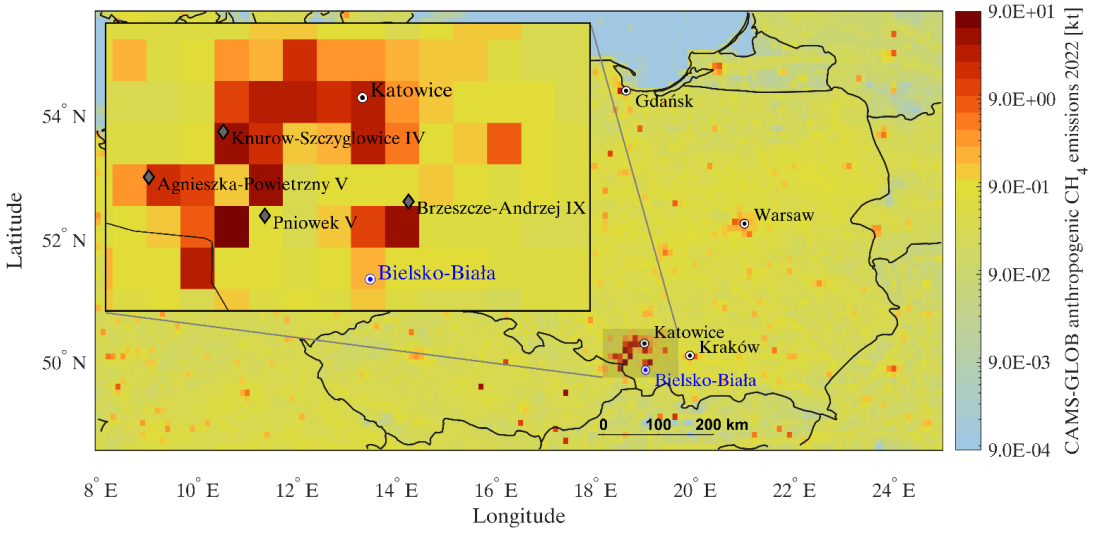

Figure 1. Total anthropogenic CH_4 emissions of Poland in 2022, based on CAMS-GLOB-ANT (Copernicus Atmosphere Monitoring Service global anthropogenic emissions, 0.1° x 0.1°, version 6.2) (Granier et al., 2019; Soulie et al., 2024), where the shaded area around Katowice represents the USCB, enlarged with the locations of the four probed coal mine ventilation shafts in the left (grey diamonds). The blue city indicates the campaign base at the Bielsko-Biała airfield. Emission data retrieved from ECCAD - the GEIA database (Emissions of atmospheric Compounds and Compilation of Ancillary Data within the Global Emissions InitiAtive) (Re3data.Org, 2023).

2.2 The HELiPOD platform and its instrumentation

The *HELiPOD* (Fig. 2) is a helicopter-towed platform for atmospheric and other environmental measurements to investigate local and regional phenomena (Pätzold et al., 2023). It provides the possibility for flight patterns on a horizontal scale of typically 100 m to 100 km and at altitudes from 50 m up to 3000 m. It has the dimensions of 5.2 m x 2.1 m x 1.2 m and a

https://doi.org/10.5194/egusphere-2025-1010
Preprint. Discussion started: 12 March 2025

weight of around 325 kg, including payload. Depending on the scientific payload and the environmental conditions, the *HELiPOD* is powered by up to two integrated 5 kWh batteries, allowing for complete power independence from the helicopter. During MTG-Poland, the carrier of the *HELiPOD* was an Eurocopter AS350 Écureuil (Fig. 2, right) of the local helicopter company Helipoland (https://helipoland.com).

To ensure turbulence-free atmospheric measurements of the *HELiPOD*, Pätzold et al. (2023) estimated the influence of the helicopter rotor wake. They compute a wake inclination angle of 6.5° for an assumed rotor thrust (equal to the helicopter plus payload weight of approx. 3.5 t and a rotor radius of 5.5 m) and a flight speed of 40 m s^{-1}, which are the approximate measurement parameters. Therefore, the wake is just striking the top of the helicopter's fuselage but is far from the rope (length of 25 m) and the attached *HELiPOD* during cruise flight (Fig. 2, right). Only during take-off and landing the *HELiPOD* is exposed to the rotor downwash for a short amount of time. The typical flight time is 2 to 3.5 hours, resulting in a total flight distance of up to 500 km.

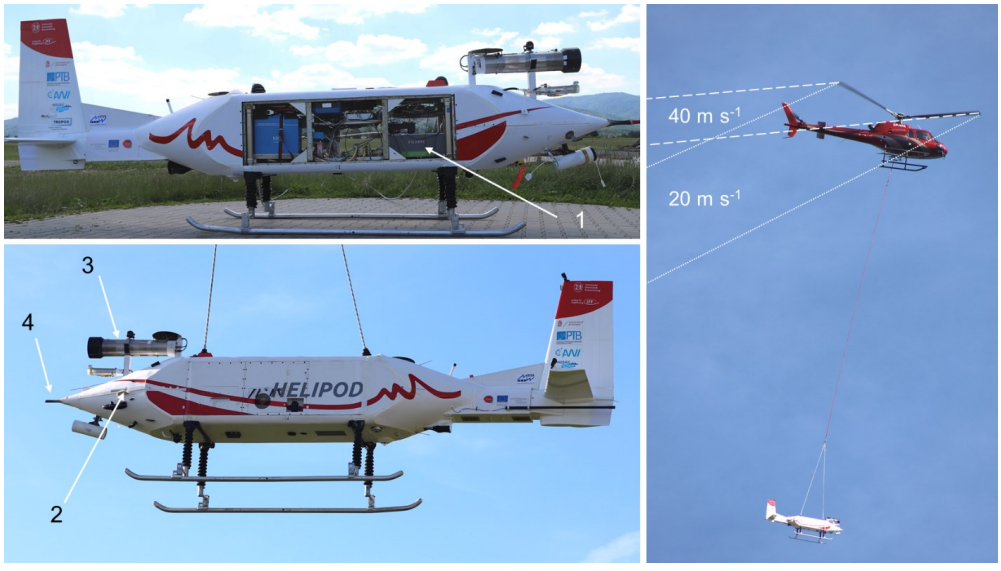

Figure 2. The helicopter-borne measurement system *HELiPOD* with instruments mounted inside and outside: Picarro G2401-m (1) with its inlet (2) for precise CH_4 measurements, Licor LI-7700 (3) for high resolution CH_4 measurements and a five-hole probe (4) for precise wind measurements. The right picture illustrates the rotor downwash area for the air speed of 20 m s^{-1} and 40 m s^{-1} (adapted from Pätzold et al., 2023).

In addition to sensors for determining position and orientation at high resolution, the *HELiPOD* is equipped with around 50 sensors relevant to five fields of research: atmospheric dynamics, trace gases, aerosols, radiation, and surface properties (Pätzold et al., 2023). However, only the parts of the instrumentation relevant for this study are introduced here.

The scientific payload installed on the *HELiPOD* during the MTG-Poland campaign consisted of a variety of instruments to measure greenhouse gases and meteorological parameters, see Table 1. To minimize risks due to instrument malfunction and to evaluate the possible impact of the CH_4 measurements on the mass flux uncertainty, we deployed two different in-situ instruments for the measurement of CH_4:

- A Picarro G2401-m was mounted inside the *HELiPOD* centre section (Fig. 2, location 1), connected with a ¼" perfluoroalkoxy alkane (PFA) tube of 1 m length to the inlet at location 2.
- A Licor LI-7700 was mounted outside on the *HELiPOD* front part (location 3).

The Picarro G2401-m, hereafter simply named as Picarro, is based on cavity ringdown spectroscopy (CRDS) (Crosson, 2008), while the Licor LI-7700, hereafter simply named as Licor, is an open path CH_4 analyser (McDermitt et al., 2011), based on spectrometric measurement in near infrared (around 1.65 µm) inside the open optical cavity (Herriot cell) with effective laser

https://doi.org/10.5194/egusphere-2025-1010
Preprint. Discussion started: 12 March 2025

beam path of 30 m. The flow rate through the Picarro is 300 standard ml min^{-1}, leading to a latency of 5 s, which has to be considered in the data post-processing.

After each mission flight, maintenance work was performed, e.g. the mirror of the Licor was cleaned due to contamination from flies, black carbon and dust, which reduced the RSSI (Residual Signal Strength Indicator) during every flight typically by 30 %. On-site CH_4 calibrations of both instruments were performed on average every second to third day using three different NOAA (National Oceanic and Atmospheric Administration) corrected Air Liquide standards with high (2690 ppb), middle (1845 ppb) and low (1625 ppb) mixing ratios. We note, that the ppm and ppb notation is widely used in the trace gas community and, although not recommended within the International System of Units (SI), we apply it here for the sake of uniformity. Hereafter, ppm and ppb refer to the mole fractions µmol mol^{-1} and nmol mol^{-1}, respectively. Laboratory calibrations with the three Air Liquide standards and two NOAA standards were performed before and after the campaigns and did not show any significant trends, deviations or outliers. Further information on the calibrations is provided in the Supplement S2.

A further important difference of the two instruments is the measurement frequency of 2 Hz (Picarro) and 40 Hz (Licor) and the respective precision of ~1 ppb and ~5 ppb, respectively. The high sampling frequencies are advantageous to adequately sample the CH_4 plumes. At the foreseen flight distances of ~400 m to 3000 m from the emitter, the plumes are typically expected to have a narrow width between ~200 m to 1 km, which translates into ~5 s to 25 s sampling time within the plume at the typical *HELiPOD* flight speed of 40 m s^{-1}.

Table 1. Overview of the *HELiPOD* sensors relevant for this study (see also Fig. 2 for the position).

Instrument	Species/Parameter	Data rate	Precision
Picarro G2401-m Cavity ringdown spectroscopy (CRDS)	CH_4 & CO_2	~ 2 Hz	~ 1 ppb
Licor LI-7700 Open path gas analyser	CH_4	40 Hz	~ 5 ppb @ 10 Hz
Meteorological sensors	Wind vector	100 Hz	0.1 m s^{-1}, 3°
	Temperature	100 Hz	0.1 K
	Humidity	100 Hz	1 % RH

During the flights, a subset of the measurement data is transferred from the *HELiPOD* via Wi-Fi to the operator's laptop in the helicopter, where it is visualised at the *HELiPOD* mission monitor. It combines a map of live data, where CH_4 and wind measurements can be chosen, a time series of selected species and vertical profiles of various parameters. This data composition allows the scientific operators in the helicopter to monitor the health status of the system and to make decisions for the next flight manoeuvres (Pätzold et al., 2023).

The three-dimensional wind vector is calculated based on the vector difference between airspeed vector and groundspeed vector. The airspeed vector is determined by combining pressure data at a five-hole probe (Fig. 2, location 4) with position and the attitude angles of the measurement platform, which are determined using a Global Navigation Satellite System aided inertial measurement unit system (GNSS-IMU-System). The wind vector is provided at a frequency of 100 Hz.

Temperature was measured with different fine wire sensors and resistance thermometers Pt100. Humidity was measured by a Lyman-Alpha instrument, different capacitive sensors, a dew point mirror and with an infrared absorption sensor Licor LI-7500RS, which also measures CO_2. The signals from the different temperature and humidity sensors were complementary filtered to increase the accuracy and temporal resolution of the measurements (see Pätzold et al. (2023) for detailed explanations). All data of the individual *HELiPOD* sensors are collected and digitized with a client-master system, and stored with precise time stamp on the data acquisition systems. Calibrations of the CH_4 sensors during the campaign and other post campaign calibrations were applied as part of the post processing. The airspeed vector measurement was calibrated in post-processing using wind calibration patterns.

https://doi.org/10.5194/egusphere-2025-1010
Preprint. Discussion started: 12 March 2025

2.3 The mass balance approach

We use the widely applied aircraft mass balance approach, described in detail in numerous publications (e.g. Cambaliza et al., 2014; Conley et al., 2017; Fiehn et al., 2020; France et al., 2021; Pühl et al., 2024), to estimate the CH_4 mass flux of the coal mine ventilation shafts. The mass flux F of a species C through a crosswind curtain downwind of an emission source is estimated by the integration of the enhancement above the background concentration $[C]_{bg}$ combined with the wind speed component of the wind $U_\perp$ perpendicular to the curtain, following Eq. 1 (e.g. Cambaliza et al., 2014):

$$F = \int_{z_0}^{z_{PBL\,top}} \int_{-x}^{x} \left([C] - [C]_{bg}\right) U_\perp dx\, dz \tag{1}$$

The parameters z_0 and z_{PBLtop} represent the vertical limits of the plume from ground to the top of the convective planetary boundary layer (PBL) and -x and +x represent the horizontal limits of the plume width from an arbitrary midpoint. The brackets around C denote the measured concentration. The full integration over the limits of the plane yields an emission rate F, in the unit kg s^{-1} or kg h^{-1}.

We use a discrete approach of Eq. 1 by calculating the mass flux F_i for pointwise CH_4 enhancements i (2 Hz and 40 Hz) during individual transects crossing the plume at different altitudes downwind of the probed emission source, following:

$$F_i = [\Delta C]_i \cdot \frac{M_{CH_4} \cdot p_i}{R \cdot T_i} \cdot U_{\perp,i} \cdot W_i \cdot H_i\,, \tag{2}$$

where F_i is the discrete mass flux for a pointwise measurement [kg s^{-1}], $[\Delta C]_i$ = $[CH_4]_i$ - $[CH_4]_{bg,i}$ is the pointwise CH_4 enhancement over the background mixing ratio [mol mol^{-1}], M is the molar mass of CH_4 [kg mol^{-1}], p_i is the air pressure [Pa], R is the universal gas constant [J mol^{-1} K^{-1}], T_i is the temperature [K], $U_{\perp,i}$ is the perpendicular component of the wind speed to the curtain [m s^{-1}], W_i is the horizontal extension of $[\Delta C_i]$ in [m], equal to the distance between two pointwise measurements, and H_i is the vertical extent of $[\Delta C_i]$ in [m]. A detailed description of the mass flux calculation is provided in the Supplement S3. Here, just a brief summary is given.

The background concentration $[CH_4]_{bg,i}$ is individually calculated for each transect and pointwise measurement i by interpolating between 10-second averages of both edges of a transect to account for gradients in the background. Methane plumes are identified by $[\Delta C]_i + 3\sigma$, were σ is the mean of the standard deviations of the 10-second average periods at both edges. In that way, we account for uncertainties in the background concentrations and can separate plumes of targeted emission sources from other sources as well. The perpendicular component of the wind speed to the curtain $U_{\perp,i}$ is calculated from the measured wind speed U_i, wind direction and *HELiPOD* heading. The horizontal extension W_i of a pointwise CH_4 enhancement is calculated based on the ground speed of the *HELiPOD* and the measurement frequency. The vertical extension H_i is estimated to reach halfway down to the next lower transect and halfway up to the next higher transect (e.g. Foulds et al., 2022; Pühl et al., 2024). If a mobile ground-based transect is available, the CH_4 enhancements at the ground and the lowest transect are estimated to reach halfway down and up, respectively. In the absence of a mobile ground-based transect, CH_4 enhancements of the lowest transect are estimated to reach to the ground. If CH_4 enhancements at the highest probed transect are still present, they are estimated to reach to the top of the PBL. The convective boundary layer height is determined by deriving the temperature inversion height in parallel to a pronounced reduction in CH_4 and water vapour. For this determination, we use measured vertical profiles of the potential temperature (θ) and its gradient $d\theta\, dz^{-1}$, H_2O and CH_4 concentrations (e.g. Cambaliza et al., 2014), which were probed at the beginning and end of each individual flight up to an altitude of 3 km. Here we note, that all given altitudes are above ground layer (AGL).

https://doi.org/10.5194/egusphere-2025-1010
Preprint. Discussion started: 12 March 2025

Finally, the pointwise mass fluxes F_i are summed up to gain the mass flux of selected plumes on a transect (if emission sources are separated). These mass fluxes are then summed up to gain mass fluxes per transect which are summed up to gain the total mass flux $F_{top\text{-}down}$ for the complete curtain. A detailed explanation in five calculation steps is provided in Supplement S3. The mass flux uncertainty is briefly addressed in Sect. 2.5 with more details being provided in Supplement S4. Mass fluxes are calculated separately for Picarro (2 Hz) and Licor (40 Hz) measurements. A comparison between both instruments revealed an excellent agreement ($R^2 = 0.99$), with the Picarro measurements generally leading to lower mass flux uncertainties (median -8 %), see Supplement S5. Therefore, the final mass flux estimate per target and flight is the average of Picarro-based mass flux estimates for up to four curtains at different distances downwind of the emission source (see Sect. 2.4).

2.4 Sampling strategy

In general, gases emitted from point sources are mixed into the PBL during daytime or stay below a pronounced inversion layer (if present) within the PBL during night time or in the winter season. Depending on the wind conditions and atmospheric stability, the plume shape of these emissions differs (e.g. Geiger et al., 1995). For an unstably stratified atmosphere and low wind speeds with variable direction, the emissions will spread in all spatial directions which hampers a straightforward analysis of the airborne measurement data. For a stably stratified atmosphere with pronounced wind speed (>3 m s^{-1}), the emissions will be advected along the prevailing wind direction and theoretically form a cone shape broadening with distance from the source. The latter case can be approximately described by a Gaussian plume model (Sykes et al., 1986; Leelőssy et al., 2014; Conley et al., 2017; Hajny et al., 2023). Hence, our measurement flights were conducted during suitable meteorological conditions. The preferred wind speed range to probe the ventilation shafts was 3 to 10 m s^{-1} to allow for an effective spread of the CH_4 plume. Depending on the wind direction and cloud forecast, the target ventilation shaft was chosen on a daily basis. The selected shaft was less impacted by other emission sources located upwind. Only days with a cloud base higher than 1 km were chosen to conform with the visual flight rules (VFR) for helicopter operations.

A typical flight pattern is shown in Fig. 3, targeting emissions of the shaft Agnieszka-Powietrzny V. Straight race tracks with a length of around 4 km to 6 km were flown perpendicular to the wind direction at different altitudes downwind of the target source to sufficiently capture the vertical and horizontal dimensions of the plume, as well as the background concentration at both edges of the plume transects (similar to e.g. Cambaliza et al., 2014; Heimburger et al., 2017; Fiehn et al., 2020).

This creates a number of 2D curtains through which the mass flux is estimated (Fig. 4 and Fig. 5). The altitudes of the transects generally range from the lowest safe flight altitude (~50 m) up to altitudes where no enhancements are detected any more (~700 m). Depending on the plume height, 5 up to 24 plume transects were flown per curtain with vertical intervals between 25 m and 75 m. Usually, a sequential probing was conducted starting from lower to higher altitudes and, if flight time remained, going back to lower altitudes again. This sequential probing ensures, that the whole plume is covered. Of these conducted transects we selected 2 to 11 transects which are temporally close to each other (probed within ~1 h) to consider approximately constant meteorological conditions (see Step 5 in Supplement S3). We conducted 1 to 4 downwind mass balance experiments (MBE) at distances of 500 m to 5000 m from the emission source, starting with the curtain closest to the emitter (Hajny et al., 2023). In that way, we are able to separate nearby sources at closer distances were the plumes have not yet mixed while having a better vertical and horizontal plume extent farther away which also enables us to study the impact on the estimates.

https://doi.org/10.5194/egusphere-2025-1010
Preprint. Discussion started: 12 March 2025

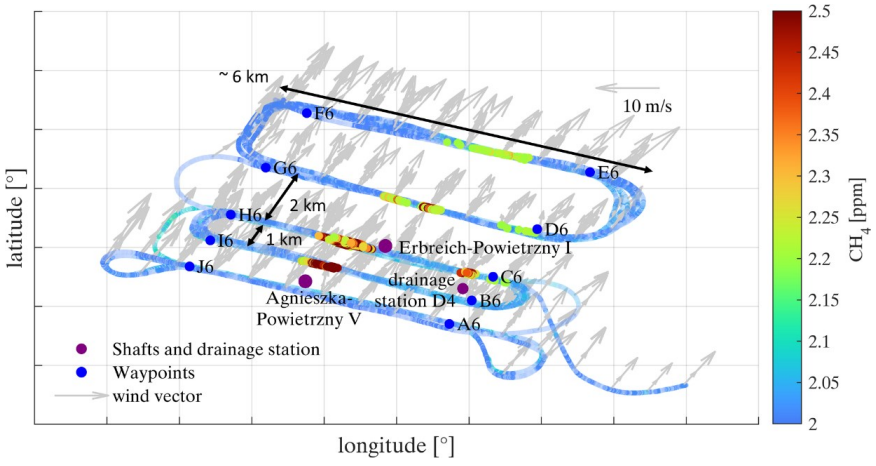

Figure 3. Top view of Flight 07 on 17 October 2022, probing the shaft Agnieszka-Powietrzny V. Additional CH_4 sources are the shaft Erbreich-Powietrzny I and the drainage station D4. All three sources are marked by purple points. Points A6 to J6 indicate the waypoints of the planned flight pattern. The wind direction was 195° to 225° (grey arrows) and nearly perpendicular to the performed mass balance experiments (MBEs).

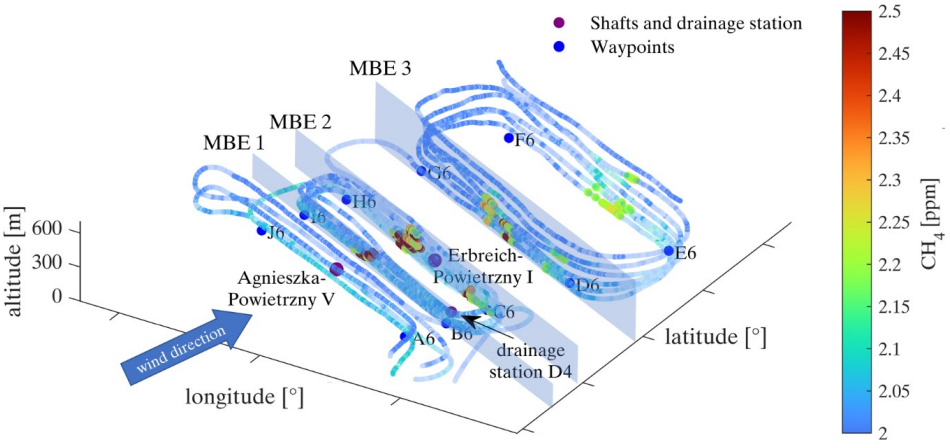

Figure 4. Cross view of Flight 07 on 17 October 2022. Three mass balance experiments (MBEs) downwind of the shafts Agnieszka-Powietrzny V, Erbreich-Powietrzny I and the drainage station D4 are selected for the calculation of CH_4 mass fluxes. Points A6 to J6 indicate the waypoints of the planned flight pattern. The upwind leg and the last downwind MBE were excluded from the calculations.

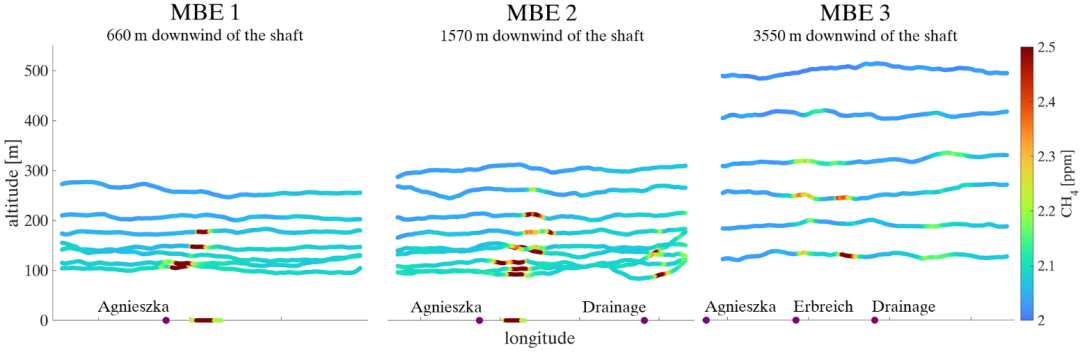

Figure 5. Selected MBEs downwind of the shaft Agnieszka-Powietrzny V, probed at different distances during Flight 07 on 17 October 2022. Clearly visible is the dispersion of the CH_4 plume with increasing distance from the source. In MBE 1 and 2, ground-based transects are included at an altitude of 0 m, conducted between MBE 1 and 2 (see Fig. S3). In MBE 2 and 3, also additional plumes from a drainage station and the shaft Erbreich-Powietrzny I are visible.

https://doi.org/10.5194/egusphere-2025-1010
Preprint. Discussion started: 12 March 2025

In the example shown in Fig. 5, MBE 1 (waypoints I6 to B6) includes only emissions of the shaft Agnieszka-Powietrzny V. Here the importance of ground-based data is also visible. Due to flight restrictions the plume could not be probed below an altitude of 100 m, which means that 50 % of the plume information of MBE 1 is missing. Especially close to the emission source, where the plume is still narrow and not well mixed, the ground-based measurements ensure a reliable mass flux estimate. This will be further discussed in Sect. 3.2.3. Additional CH_4 emissions from a drainage station and the shaft Erbreich-Powietrzny I (no explicit targets) were present starting with MBE 2 (waypoints H6 to C6) and MBE 3 (waypoints G6 to D6), respectively. The CH_4 background concentration at the transect edges of MBE 1 is ~60 ppb higher compared to MBE 3. The reason could be night time accumulation below a surface inversion layer close to the source. For the mass flux calculation, only MBE 1, 2 and 3 are selected, since at the fourth MBE emissions are already strongly mixed and are not distinguishable. The vertical dispersion of the emission plume from the shaft Agnieszka-Powietrzny V is clearly visible in the three MBEs probed at the distances of 660 m, 1570 m and 3550 m from the source (Fig. 5).

Generally, the choice of suitable probing distances highly depends on the strength of the emission source, the wind speed, atmospheric stability (Conley et al., 2017), as well as on the precision and temporal resolution of the instrument(s). Our race track distances are within the range of other aircraft-based mass balance approaches probing emissions of single point sources. Conley et al. (2017) probed at a distance of 1.5 km, Hajny et al. (2023) within 5 km, Pühl et al. (2024) at 2 to 7 km and Heimburger et al. (2017) and Fiehn et al. (2020) at a distance of ~30 km from the emission source. Additionally, we flew an upwind curtain at 3 to 4 different altitudes to identify possible upstream sources (not shown).

Flights were conducted mainly in the late morning until the early afternoon, when the PBL is well developed (Cambaliza et al., 2014; Heimburger et al., 2017) and wind speeds increase and disperse nocturnal accumulations. The duration of a mission flight varied between 2 to 3.5 hours. The *HELiPOD* air speed is ~40 m s^{-1} and thus considerably lower compared to other aircraft-based mass balance approaches, which are usually conducted at an airspeed of 60 to 70 m s^{-1} (Cambaliza et al., 2014; Conley et al., 2017; France et al., 2021; Hajny et al., 2023). In that way, the spatial resolution of the measurements is higher (0.4 m, 1 m and 20 m for measurement frequencies of 100 Hz, 40 Hz and 2 Hz), allowing for spatially closer probing and hence more reliable source separation in a complex emission environment.

In summary, ten *HELiPOD* mission flights were conducted within the time period from 14–23 June 2022 and nine mission flights from 11–18 October 2022 probing four different coal mine ventilation shafts in the USCB region (see Table 2 and for more detailed information Supplement S1). The last two flights in October were dedicated to a controlled CH_4 release experiment at the Bielsko-Biała airfield (see Sect. 2.8).

Table 2. Number of *HELiPOD* mission flights to the different targets during the METHANE-To-Go-Poland field campaign in June and October 2022.

Source	Name	June 2022	October 2022	Total flights
Shaft 1	Knurow-Szczyglowice IV	5	-	5
Shaft 2	Brzeszcze-Andrzej IX	3	2	5
Shaft 3	Pniowek V	2	3	5
Shaft 4	Agnieszka-Powietrzny V	-	2	2
	Controlled release	-	2	2
Total flights		10	9	19

2.5 Estimating the mass flux uncertainty

The mass flux uncertainty F_{unc} (Eq. 3) consists of three parts: i) F_{unc_flux} from the flux calculation (Eq. 2) via Gaussian error propagation, ii) F_{unc_bottom} from the extrapolation of the lowest probed transect to the ground and iii) F_{unc_top} from the

https://doi.org/10.5194/egusphere-2025-1010
Preprint. Discussion started: 12 March 2025

extrapolation of the highest probed transect to the estimated top of the plume. We use this more conservative uncertainty estimate due to the closer probing to emission sources where the plume is not yet well mixed in the PBL.

$$F_{unc} = F_{unc\_flux} + F_{unc\_bottom} + F_{unc\_top} \quad (3)$$

The uncertainty F_{unc_flux} is obtained by summing up pointwise measurement uncertainties $F_{i_{unc\_flux}}$ (Eq. 4) derived by Gaussian error propagation of Eq. 2 for identified plumes on selected transects, similar to the calculation of the total mass flux (see Sect 2.3, also for the description of the parameters in Eq. 4). Detailed information on the errors σ of each parameter in Eq. 4 is provided in the Supplement S4.

$$F_{i_{unc\_flux}} = \sqrt{\left(\frac{\partial F_i}{\partial [\Delta C]_i} \cdot \sigma_{[\Delta C]}\right)^2 + \left(\frac{\partial F_i}{\partial p_i} \cdot \sigma_{\mathrm{p}}\right)^2 + \left(\frac{\partial F_i}{\partial T_i} \cdot \sigma_{\mathrm{T}}\right)^2 + \left(\frac{\partial F_i}{\partial U_i} \cdot \sigma_{\mathrm{U}}\right)^2 + \left(\frac{\partial F_i}{\partial W_i} \cdot \sigma_{\mathrm{W}}\right)^2} \quad (4)$$

The Uncertainty of the plume height is considered separately. For the height of individual layers around the transect, no uncertainty is specified. Instead, we calculate mass flux uncertainties introduced by the altitude uncertainty of the top of the plume and the plume extrapolation to the ground (only if no ground-based data are available). F_{unc_top} is the mass flux uncertainty introduced by the estimated altitude of the top of the plume. We estimate the uncertainty of the top of the plume to be half the distance from the highest transect with CH_4 enhancements to the next higher transect without CH_4 enhancement (if applicable). From this distance *H*, F_{unc_top} is calculated (see example in Supplement S4). If the probed transect at the highest altitude still shows CH_4 enhancements, the uncertainty of the top of the plume is estimated to be half the distance from this transect until the altitude of the next higher inversion layer or until the PBL. F_{unc_bottom} is the mass flux uncertainty introduced by extrapolating the plume from the lowest transect to the ground. If no ground-based data are available, the uncertainty of the lower plume limit is estimated to be half the distance from the lowest probed transect to the ground. From this distance *H*, F_{unc_bottom} is calculated. If ground-based data are available, $F_{unc\_bottom} = 0$.

2.6 Supportive ground-based measurements

The helicopter-borne MTG-Poland team was accompanied by further research teams carrying out ground-based measurements in the same area and at the same time, most notably mobile CH_4 in-situ measurements carried out by the University of Krakow (AGH) (Jagoda et al., 2024). The helicopter-borne team was partly guided by on-site reports of those teams by receiving the latest live observations via mobile phone.

In this study, the mobile ground-based measurements of AGH are used to complement the airborne CH_4 measurements for the mass flux estimate at the lower altitudes up to 100 m, which are partly not covered by the *HELiPOD*. AGH performed mobile CH_4 measurements by car equipped with a Licor 7810 and a Picarro G2201-i with recording frequencies of 1 Hz and 0.25 Hz, respectively. The measurements were synchronized with GPS position data and wind data from a Gill WindSonic 60 anemometer at 1 Hz. Mobile ground-based data are added to the mass flux calculation, if they properly transect through the CH_4 plume and if the measurements are close in time (< 1 h) and space (mean distance < 500 m) to the *HELiPOD* flight tracks. Further measurements performed by the University of Heidelberg, Technische Universität of Munich, Technische Universität of Braunschweig and Swiss Federal Laboratories for Materials Science and Technology (EMPA), which are not part of this study, will be summarized in a synthesis paper.

2.7 Methane safety sensor data of coal mine ventilation shafts

To ensure a safe underground work environment, hard coal mines have to implement control methods to maintain CH_4 concentrations in the return air flowing from the excavation area below 1.5 % (Journal of Laws, 2017). Ventilation systems supply sufficient air to move and dilute more concentrated CH_4 in-mine air that is generated from the gas emission zone. Sometimes an accompanying CH_4 drainage system is used (see scheme in Fig. 6) to directly remove CH_4 before it enters the

https://doi.org/10.5194/egusphere-2025-1010
Preprint. Discussion started: 12 March 2025

ventilation system. The general principle of CH_4 capturing consists of draining it from coal seams and surrounding rock through specially designed boreholes. Later, the gas is discharged via a separate system of pipelines onto the surface, utilizing the low pressure generated in a CH_4 drainage station (Swolkień, 2015). For hard coal with a relatively low gas content, drainage is technically challenging and economically infeasible, hence, CH_4 is emitted directly into the atmosphere by using only a ventilation system (Fig. 6). A drainage system is mostly used in mines with high CH_4 emissions, where the air supply to the excavation is generally insufficient to reduce CH_4 concentrations to a safe level. When not vented Polish coal mines use the drained CH_4 either internally or sell it to external power plants. However, according to the Polish State Mining Authority (WUG), the average drainage efficiency of capturing CH_4 is only 39 % in Poland, hence ventilation shafts release the remaining 61 % directly into the atmosphere (WUG, 2023). Of this 39 %, the average CH_4 utilisation efficiency is about 68 %. As such nearly a third of the CH_4 captured by the drainage stations is released into the atmosphere (WUG, 2023). In Poland, drainage stations are therefore non-negligible CH_4 emission sources, which account on average for 12.5 % of the total annual CH_4 emissions of underground coal mines (Swolkień et al., 2022).

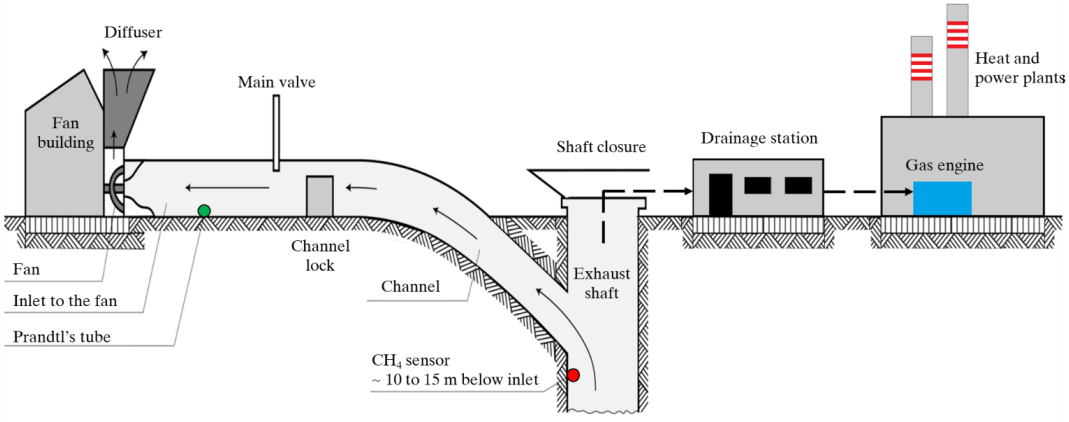

Figure 6. Scheme of a coal mine ventilation shaft and optional drainage station. The position of the CH_4 safety sensor is indicated by the red point inside the shaft, and the position of the Prandtl´s tube is indicated by the green point inside the channel. Adapted from Swolkień (2020) and Andersen et al., (2023).

The CH_4 concentrations in the ventilation shafts are monitored with an EMAG-Serwis-type DCH sensor (**D**etector **CH**$_4$, EMAG Service: https://emagserwis.pl/produkty/metanomierze/, last access: 27 January 2025). This sensor (measurement range 0 to 100%, uncertainty 0.1 %) is part of the automatic coal mine gas measurement systems and is placed 10 to 15 m down into the exhaust shaft (Andersen et al., 2023), as shown in Fig. 6. The air flow rate in the ventilation channel is measured using a Prandtl tube (Fig. 6, green point) located between the main valve and the fan (Swolkień et al., 2022). The uncertainty of the Prandtl tube is 100 m³ min^{-1}. For the calculation of the total air flow, also flow losses are considered, which are typically in the range of 2 to 33 % of the measured air flow in the ventilation channel. These losses are calculated by the mine operators as the difference between the stream measured with the Prandtl tube in the channel and the stream measured at the bottom of the mine at the shaft inlet. The CH_4 emission rate [kg h^{-1}] is calculated following Eq. 5:

$$F_{bottom-up} = [\mathrm{CH_4}] \cdot \frac{M_{CH_4} \cdot p_{shaft}}{R \cdot T_{shaft}} \cdot V_{shaft} \quad (5)$$

where [CH_4] is the measured CH_4 concentration [%], p is the pressure in the shaft [Pa], M_{CH4} is the molar mass of CH_4 [g mol^{-1}] (16.043 g mol^{-1}), R is the universal gas constant [J mol^{-1} K^{-1}], T_{shaft} is the temperature in the shaft [K] and V_{shaft} is the air flow rate [m^3 min^{-1}]. The air temperature in the shafts ranges between 18 °C to 23 °C and the pressure between 967 hPa to 983 hPa. The emission rates are calculated from the raw CH_4 concentration and air flow rate measurements obtained every minute within each specific ventilation shaft for the time of the helicopter-borne measurements. The relative uncertainty of the

https://doi.org/10.5194/egusphere-2025-1010
Preprint. Discussion started: 12 March 2025

emission estimates ranges from 14 % to 55 %. Industry data on the drained CH_4 is proprietary and not publicly available (Swolkień et al., 2022).

2.8 Set-up of a controlled CH_4 release experiment

Controlled release experiments are a typical tool to assess the mass flux quantification method and flight strategy (e.g. Morales et al., 2022). On 17 and 18 October 2022, two flights were dedicated to such a controlled CH_4 release experiment, which was set up at the Bielsko-Biała airfield. CH_4 was constantly released from an altitude of ~7 m above the ground in the southwest part of the airfield. The outlet was connected via a Bronkhorst mass flow controller to three 50 l gas bottles filled with 200 bar at the beginning (Air Liquide CH_4 2.5 with a purity >99.5 %). The release rate was ~21 kg h^{-1} ± 0.5 kg h^{-1} CH_4 during both experiments. The releases started at 12:37 UTC on 17 October 2022 and 9:37 UTC on 18 October 2022 with a duration of 57 min and 41 min, respectively. Measurements were conducted with the helicopter flying at low altitude directly above the runway, perpendicular to the wind direction (~ 200°) and 300 m to 400 m downwind of the release point. This special set-up allowed probing at altitudes as low as ~5 m above the runway ground. Additional mobile ground-based measurements were performed around and inside the fenced area of the airport. The primary objective of the experiment was to test the ability of the helicopter-borne approach to detect CH_4 from sources with small emission rates. Detailed information on the controlled release experiment is provided in Supplement S6.

3 Results and discussion

Here we show and discuss the comparison of the top-down mass flux estimates versus bottom-up estimates using in-mine data (Sect. 3.1), a sensitivity analysis of parameters which might influence the uncertainty and accuracy of our mass flux estimates (Sect. 3.2) and the results of the controlled released experiment (Sect. 3.3). As discussed in Sect. 2.3, all presented results are based on 2 Hz Picarro CH_4 measurements.

3.1 Comparison with in-mine data

Bottom-up inventory estimates are often compared with top-down measurements as a validation approach aimed at improving the quality of bottom-up inventories. For the coal sector inventory estimates are often annual averages using calculations that amalgamate contributions from different sources by using standardized emission factors upon reported coal production (Karacan et al., 2024). Given the uncertainties of comparing with annual inventory estimates, that are in any case unavailable at the mine level in Poland, and that are not specific to ventilation air methane or drainage station sources, we take a different approach. We use bottom-up estimates from in-mine data that is time synchronized to our *HELiPOD* measurements. The quality of data from in-mine CH_4 safety sensor (Pellistor device) measurements has been recently evaluated through comparison to TDLAS (Tunable Diode Laser Absorption Spectroscopy) measurements set up by AGH (Nęcki et al., in prep. for AMT), which were performed in the ventilation shafts. Results of this experiment revealed that bottom-up estimates based on the CH_4 safety sensors and on the TDLAS measurements show a difference of less than 100 kg h^{-1}, if proper calibration routines are applied. Within an uncertainty band of 14 to 55 %, we consider the bottom-up measurements from in-mine data therefore as reliable and use them as comparator to evaluate the *HELiPOD* flux quantifications.

Out of our 59 curtains performed in total, 51 can be used for reliable MBE analyses. The remaining eight curtains showed a strong mixing with emissions from multiple sources from in- and outside the probing area and hence, were not included for further analysis. Figure 7 shows a comparison of estimated top-down mean mass fluxes and the bottom-up in-mine estimates for all shafts measured in June and October 2022, including uncertainties. Further details of the different top-down estimates are listed in Table 3.

https://doi.org/10.5194/egusphere-2025-1010
Preprint. Discussion started: 12 March 2025

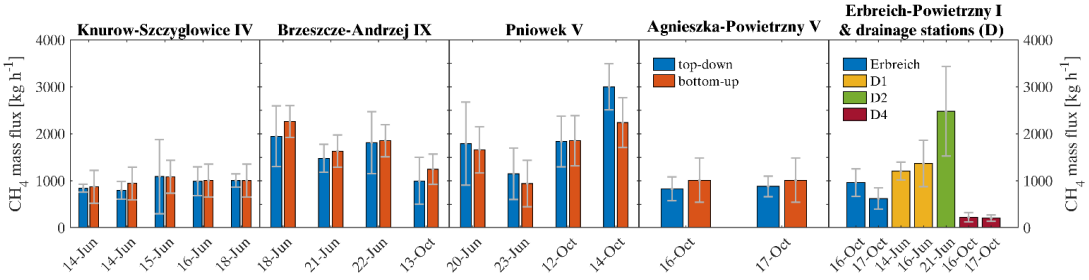

Figure 7. Estimated top-down mean mass fluxes in comparison to in-mine bottom-up estimates for all MTG-Poland flights, sorted into the four targeted shafts. Additionally, emission rates of a fifth shaft (Erbreich-Powietrzny I) and three drainage stations D1, D2 and D4, close to Knurow-Szczyglowice IV, Brzeszcze-Andrzej IX and Agnieszka-Powietrzny V, respectively, are calculated.

455

Table 3. Summary of mass flux estimates from MTG-Poland and the comparison to bottom-up in-mine estimates. Mean fluxes and uncertainties are based on single MBE estimates for the respective *HELiPOD* flights. Mean fluxes of the bottom-up in-mine estimates are matched with the flight time period of each *HELiPOD* flight. FF is the wind speed, DD is the wind direction, Ø is the average for all plumes of the mass balance experiment and σ is the root-mean-square error. Shaft 1 (Knurow-Szczyglowice IV), Shaft 2 (Brzeszcze-Andrzej IX),
460 Shaft 3 (Pniowek V) and Shaft 4 (Agnieszka-Powietrzny V) are the planned targets with available in-mine data. Shaft 5 (Erbreich-Powietrzny I) and the drainage stations D1, D2 and D4 (close to Shafts 1, 2 and 4, respectively) are additionally quantified and separately listed. The last rows list the average (except for the column MBEs, which is the sum) for 40 MBEs of Shafts 1 to 4 and for the 11 additional MBEs from Shaft 5 and drainage stations D1, D2 and D4. The average of the uncertainties is calculated using the geometric average. Estimates for every performed MBE with detailed information is provided in Table S6 to Table S11 in Supplement S7.

											Top-down		In-mine data		
Shaft	Date	take-off UTC	Flight	MBEs	MBE distances to source [m]	Ø FF [m s^{-1}]	Ø DD [°]	σ DD [°]	Ø Top of plume [m]	Top of inversion [m]	Mean flux [kg h^{-1}]	unc. [kg h^{-1}]	Mean flux [kg h^{-1}]	unc. [kg h^{-1}]	Deviation to in-mine [%]
1	14.06.2022	07:15	F03	1	1050	4.8	285	19	380	380	**841**	83	**874**	349	-4
1	14.06.2022	12:15	F04	3	790, 790, 1490	5.2	307	16	334	400	**799**	189	**945**	349	-18
1	15.06.2022	08:10	F05	3	760, 760, 1590	1.4	67	91	350	350	**1090**	793	**1086**	349	0
1	16.06.2022	07:50	F06	2	1020, 2850	6.8	222	12	406	470	**991**	305	**1008**	349	-2
1	18.06.2022	07:00	F07	3	430, 990, 990	5.5	215	14	322	500	**1006**	141	**1006**	349	0
2	18.06.2022	12:00	F08	4	960, 960, 1400, 1400	5.5	241	15	525	600	**1950**	646	**2263**	338	-16
2	21.06.2022	15:00	F10	3	470, 1080, 2350	6.9	299	9	290	290	**1480**	299	**1634**	341	-10
2	22.06.2022	08:30	F12	3	480, 480, 1080	3.2	324	29	488	600	**1813**	662	**1852**	341	-2
2	13.10.2022	11:35	F04	1	460	1.1	359	84	550	550	**998**	499	**1247**	324	-25
3	20.06.2022	06:00	F09	3	560, 1010, 1620	2.3	223	53	282	450	**1790**	885	**1662**	492	7
3	23.06.2022	06:00	F13	2	1390, 2170	1.2	82	48	190	500	**1150**	549	**942**	492	18
3	12.10.2022	09:00	F03	3	1250, 3140, 3140	3.9	76	14	433	900	**1837**	541	**1853**	532	-1
3	14.10.2022	08:00	F05	3	1290, 2870, 6600	6.1	231	10	452	600	**3000**	492	**2241**	532	25
4	16.10.2022	10:10	F06	4	670, 1560, 2660, 3660	8.2	213	8	238	440	**828**	254	**1011**	470	-22
4	17.10.2022	08:00	F07	2	660, 1570	5.9	212	10	247	490	**881**	218	**1011**	470	-15
				∑40		5.0		29	366	501	**1355**	497	**1376**	413	
5	16.10.2022	10:10	F06	3	2660, 3660, 5880	7.5	217	8	473	500	**960**	295			
5	17.10.2022	08:00	F07	1	3550	5.4	210	10	490	490	**622**	227			
D1	14.06.2022	12:15	F04	1	1490	5.3	312	16	313	400	**1210**	191			
D1	16.06.2022	07:50	F06	1	2850	7.1	228	10	470	500	**1370**	494			
D2	21.06.2022	15:00	F10	2	1900, 2460	5.4	297	12	211	300	**2480**	955			
D4	16.10.2022	10:10	F06	1	2660	7.1	210	9	411	500	**224**	100			
D4	17.10.2022	08:00	F07	2	3550, 3550	5.2	209	11	351	490	**207**	69			
				∑11		6.1		11	388	454	**1010**	438			

465

The uncertainty for the top-down estimates ranges between 13 % and 73 % (median 31 %) and of the bottom-up estimates between 15 % and 55 % (median 32 %). For quantifying the bias of our MBE approach we calculate the mean error (ME) between the top-down and bottom-up estimates (Hajny et al., 2023), following Eq. 6:

$$ME = \frac{\sum(TD_i - BU_i)}{N}, \quad (6)$$

where TD_i is the top-down emission rate per flight, BU_i is the corresponding bottom-up emission rate, and N is the number of
470 flights. In addition, we performed a paired t-test to compare the means of the top-down and bottom-up estimates (Student, 1908; Hsu and Lachenbruch, 2014). The ME between top-down and bottom-up mass fluxes is -12 ± 32 kg h^{-1} and the paired t-test indicates that the means are equal (p-value = 0.86), hence there is no statistically significant bias. As mentioned above,

https://doi.org/10.5194/egusphere-2025-1010
Preprint. Discussion started: 12 March 2025

we assume that the bottom-up in-mine data are reliable within their uncertainty range and we conclude that the helicopter-based approach is capable of reliably quantifying point source emission down to at least ~200 kg h^{-1} (emission rate of drainage station D4). However, individual mass fluxes of single MBEs may differ e.g. due to changing stability conditions of the atmosphere, causing different dynamical behaviour of the plume, or simply due to the influence of other emission sources (Table S3 in the Supplement S3 lists detailed calculations of three MBEs for a flight in October). The reason of the surprisingly good agreement might be first our sophisticated flight strategy with multiple MBEs in different distances of the source and multiple vertical transects covering in most cases the lower and upper edge of the plume. Second, the estimated emission rates of the ventilation shafts based on the bottom up in-mine data are relatively consistent during the time period that *HELiPOD* measurements were performed and this indicates that emission rates did not significantly vary during individual flights.

Due to the ability of our helicopter-borne method to separate nearby emission sources, we could estimate emission rates of four additional sources from 11 MBEs: one further ventilation shaft and three drainage stations. The fifth shaft Erbreich-Powietrzny I and two of the drainage stations were probed at two different days, showing similar emission rates within the uncertainty range (Table 3). Of note are the emission rates of the drainage stations D1 and D2, which have the same order of magnitude as the corresponding ventilation shafts, in fact D2 emissions exceed that of the corresponding ventilation shaft. Here we provide the first measurements that serve as independent estimates of CH_4 emissions from drainage stations in Poland. This is of particular importance because emission rates of ventilation shafts and drainage stations are typically reported as a sum that represents the total for a given coal mine. Andersen et al. (2021) note that the WUG reports that the ratio of emissions from ventilation versus drainage sources is 4:1. While ventilation shaft emissions are continuous, although variability is not well known, those from drainage stations may be more intermittent and variable. When the corresponding emissions from three coal mines of the ventilation shafts (Knurow-Szczyglowice IV, Brzeszcze-Andrzej IX and Agnieszka-Powietrzny V) and drainage stations (D1, D2 and D4, respectively) are compared a 1:1 ratio is evident. The finding of broadly equivalent average emissions from the three ventilation shafts (~1,152 kg h^{-1}) and corresponding drainage stations (~1,089 kg h^{-1}) indicates that more attention needs to be given to the latter source. In the future, the measurement of drainage station emissions might become even more important, since they constitute an additional point source which, for the purposes of verification using top-down methods, should be reported separately.

3.2 Sensitivity Studies

To better understand the parameters that influence the production of a reliable mass flux estimate of our helicopter-borne method, several sensitivity analyses were performed. In the next subsection, we analyse and address uncertainty and closeness to the in-mine data as related to wind speed and direction, the horizontal/vertical probing density and the impact of including mobile ground-based measurements.

3.2.1 Impact of wind speed and direction

Figure 8a shows the relative mass flux uncertainty (F_{unc}/F in percent) as defined by the wind conditions during the measurement of MBEs. Wind speed and the variation of the wind direction have a clear impact on the relative mass flux uncertainty. The mass flux uncertainty starts to increase when the wind speed decreases below 3.5 m s^{-1} and also when the wind direction variation increases to more than 30°, which naturally correlates with low wind speed. Figure 8b shows the relative deviation of the top-down to the bottom-up estimate in relation to the bottom-up estimate ($|F_{top-down} - F_{bottom-up}|/F_{bottom-up}$ in percent) in dependency of the wind conditions. Surprisingly, at low wind speed the relative deviation between the two estimates stays below ~30 %. Above 5 m s^{-1} the spread of the deviations is larger, potentially caused by probing a smaller plume cross section (due to the narrower plume shape at larger wind speed) and hence less measurement points within the plume. However, the deviations above 50 % belong to two distinct flights (Flight 8 in June and Flight 5 in October) and seem to have no clear

https://doi.org/10.5194/egusphere-2025-1010
Preprint. Discussion started: 12 March 2025

influence from other meteorological parameters or with the flight strategy and are therefore considered to be outliers. Hence, Figure 8b indicates that accurate MBEs might also be performed at low wind speed, just with higher underlying uncertainties. During higher wind speeds and steady wind direction, it might be advantageous in future campaigns to probe plumes not perpendicular to the wind direction but with an angle of e.g. 30 degrees. This enlarges the cross section through plumes, especially when flying close to the emission source, and hence the probing time which can lead to more accurate mass flux estimates.

3.2.2 Density of probing

During MTG-Poland, the number of incorporated transects per MBE varied between 2 and 11 (see Sect. 2.4). The vertical distance between the transects ranged from 30 m to 130 m (on average 72 m). Figure 9a shows the relative mass flux uncertainty in dependency of the number of incorporated transects per MBE. As expected this indicates a slight decrease of the uncertainty with increasing number of transects. However, with more than five transects the relative uncertainty stays below 50 %, i.e. 5 to 6 incorporated transects are sufficient (e.g. Tettenborn et al., 2025). Surprisingly, the relative deviation between the top-down and the bottom-up estimates seems to be less impacted by the number of transects (Fig. 9b).

Furthermore, flying multiple MBEs downwind of the emission source increases the agreement between top-down and bottom-up mass flux estimates (Fig. 10). Mean mass fluxes of 2 to 4 performed MBEs per flight and target show a better agreement to in-mine data (Fig. 10b) compared to single MBEs which have a larger spread around the 1:1 line (Fig. 10a). Therefore, we recommend to conduct two or more MBEs at distances of 500 m to 5000 m with the *HELiPOD* to gain a statistically robust mean mass flux estimate.

In further sensitivity studies, we also investigated the mass flux uncertainty and the deviation of top-down to bottom-up estimates depending on i) the distance of the MBEs from the emission source, ii) the altitude of the lowest transect, iii) the altitude of the highest transect and iv) the time of probing (see Supplement S5). For point i) we conclude that there is no specific optimal distance, but a preferred distance range of ~500 m to 5000 m (according to wind speed and instrument precision) in which MBEs with the *HELiPOD* set-up should be conducted. The results indicate for point ii) that a lower height of the highest transect is associated with a higher mass flux uncertainty. And for point iii) that the mass flux uncertainty tends to slightly increase with increasing altitude of the lowest transect. By contrast, for the time of probing we found no large difference for either uncertainty or comparability of estimates.

3.2.3 In- and excluding mobile ground-based measurements

Mobile ground-based measurements complemented the helicopter-borne measurements and deliver important information for the lowest part of the plume. This is of particular importance when the lowest *HELiPOD* transect is higher than 100 m and/or the flight tracks are close to the emission source. Here, the plume is not yet well mixed and more than 50 % of the plume might not be covered by the flown transects. If a co-located mobile ground-based transect is available for a specific MBE, the enhancements at the ground are estimated to reach halfway up to the lowest *HELiPOD* transect, which is also estimated to reach halfway down to the ground. Without a mobile ground-based transect, enhancements of the lowest *HELiPOD* transect are simply estimated to reach to the ground, which may introduce an over- or underestimation. Therefore, single ground-based transects might have a large impact on the total mass flux estimate when flying close to the emission source.

https://doi.org/10.5194/egusphere-2025-1010
Preprint. Discussion started: 12 March 2025

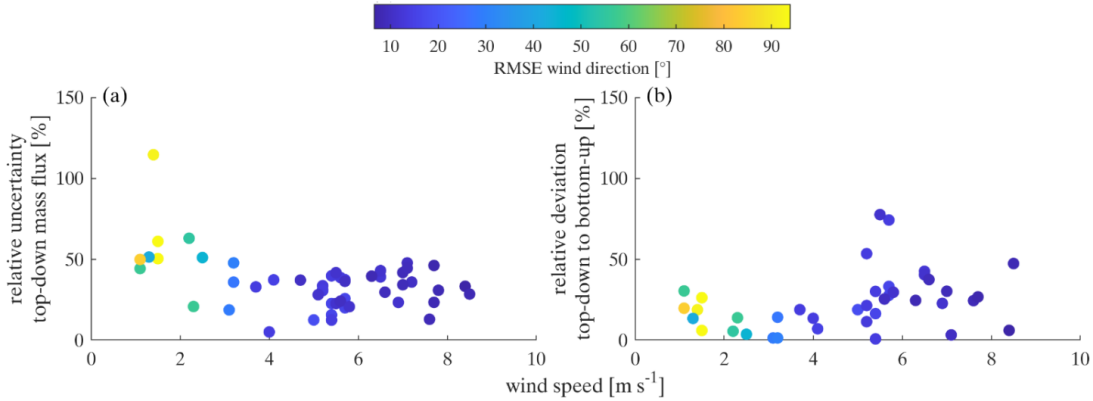

Figure 8. (a) Relative mass flux uncertainty and **(b)** relative deviation of top-down to bottom-up mass fluxes in dependency of the wind speed, colour-coded with the root-mean-square-error (RMSE) of the wind direction. This analysis includes 51 MBEs of our four targeted ventilation shafts for the relative uncertainty and 40 MBEs for the relative deviation to the in-mine data, based on Picarro measurements.

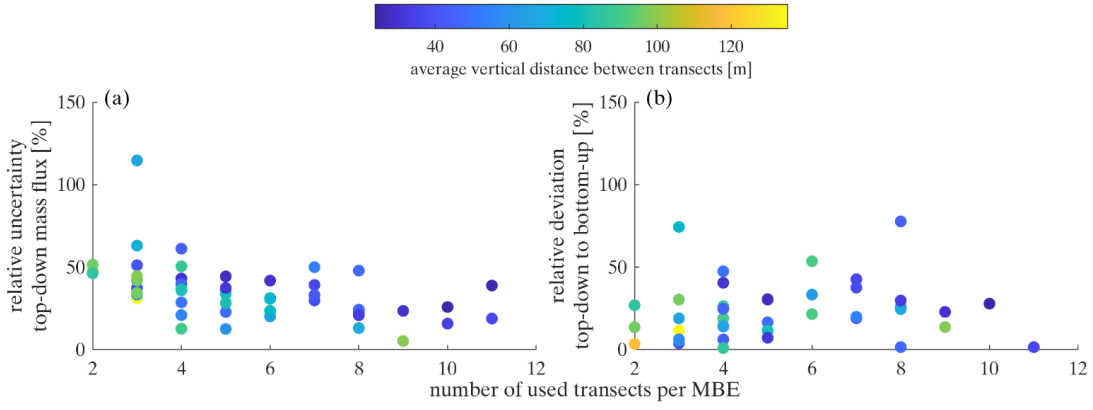

Figure 9. (a) Relative mass flux uncertainty and **(b)** relative deviation of top-down to bottom-up mass fluxes in dependency of the number of performed transects per MBE, colour-coded with the average vertical distance between transects. This analysis includes 51 MBEs of our four targeted ventilation shafts for the relative uncertainty and 40 MBEs for the relative deviation to the in-mine data, based on Picarro measurements.

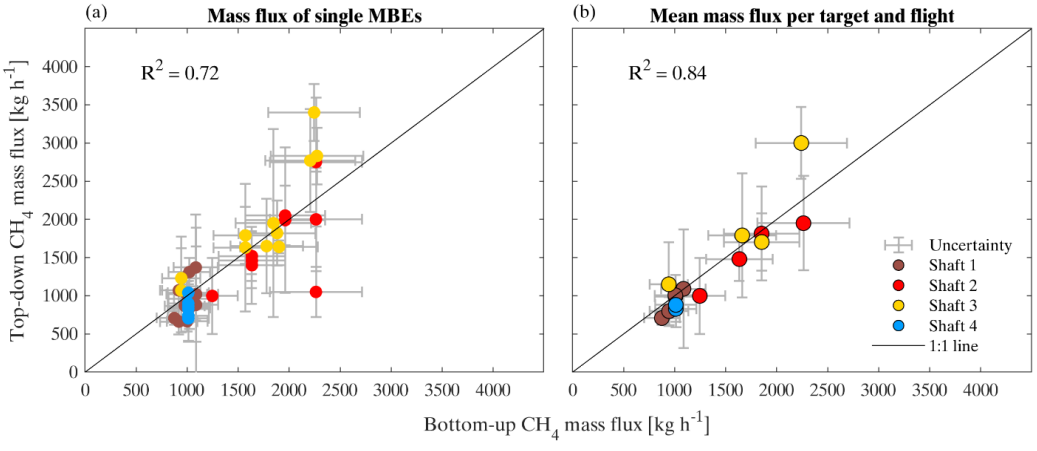

Figure 10. Bottom-up estimates from in-mine data versus estimated top-down CH_4 mass fluxes, **(a)** for 40 single MBEs of 2 Hz Picarro measurements and **(b)** for the mean per flight and target.

https://doi.org/10.5194/egusphere-2025-1010
Preprint. Discussion started: 12 March 2025

Figure 11 shows that mass flux estimates including mobile ground-based transects agree better with reported bottom-up mass fluxes based on the in-mine data. Mass fluxes in the absence of mobile ground-based transects show a mean deviation of 38 % to the in-mine data, whereas mass fluxes including mobile ground-based transects have only a mean deviation of 20 %.

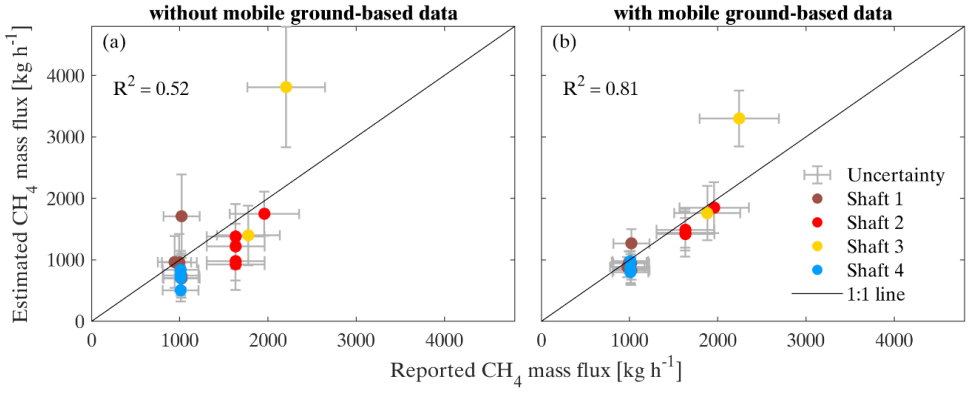

Figure 11. Reported bottom-up vs. estimated top-down mass fluxes **(a)** without mobile ground-based and **(b)** with mobile ground-based measurements. This analysis includes 15 MBEs based on airborne and mobile ground-based Licor 7810 measurements.

Ground-based data was included when the car track properly transect through the entire CH_4 ground plume, ensuring an enclosed peak with CH_4 background measurements on both edges. Furthermore, the ground-based measurements must be located close to the *HELiPOD* flight track in time (<1 h) and space (mean distance <500 m). Due to the irregular road system it was often difficult to synchronize the *HELiPOD* measurements to complete and co-located ground-based transects, leading to a successful integration of 15 out of 51 MBEs. For future *HELiPOD* field experiments where strong emission sources (>500 kg h^{-1}) in distances of <1 km are probed, it is highly recommended to perform co-located mobile ground-based measurements below or close to the flight track whenever possible (as already proposed by Fiehn et al., 2020). Here we note, that for aircraft which usually fly farther away from emission sources and also at a higher altitude, this might not apply since the plume has already mixed in the PBL and the majority of the CH_4 plume is located between >100 m and the top of the PBL or an inversion layer.

We conclude that reliable mass flux estimates with moderate uncertainties (< 50 %) can be achieved by helicopter-borne measurements when probing at least 5 to 6 transects for more than two MBEs at distances of 500 m to 5000 m and at wind speeds larger than 3 m s^{-1}. Close to emission sources, including mobile ground-based measurements helps to improve the accuracy of the mass flux estimate.

3.3 Controlled release experiment

The primary objective of the controlled release was to test if the helicopter-borne approach is also able to detect CH_4 from sources with a low emission rate. This was successfully achieved, as shown in Fig. 12 for Release 1 (17 October, 12:37–13:34 local time) and Release 2 (18 October, 09:37–10:18 local time) with CH_4 enhancements of up to 1 ppm (2 Hz Picarro) above the atmospheric background concentration of ~2 ppm. A detailed description and analyses are provided in the Supplement S6. Here a brief summary is given.

The probing conditions were mostly comparable during both experiments with wind speed of 4 m s^{-1} to 6 m s^{-1} and a wind direction of 200° to 225° (see Fig. S14 in Supplement S6). The total released amount of CH_4 was 21.2 kg h^{-1} ± 0.5 kg h^{-1} (Release 1) and 21.3 kg h^{-1} ± 0.5 kg h^{-1} (Release 2). The cross sections in Fig. 12 show that, compared to the conducted MBEs for the ventilation shafts (Fig. 5), the flight altitude changes during the plume crossing and that multiple overlaying transects were conducted (Fig. 12). In this case, the approach introduced in Sect. 2.3 and Sect. 2.4 might not result in correct mass flux

https://doi.org/10.5194/egusphere-2025-1010
Preprint. Discussion started: 12 March 2025

estimates, when applied in the same way. Therefore, we additionally applied a binning and a single-transect approach to estimate the mass flux during the release experiment, which are both described in detail in Supplement S6.

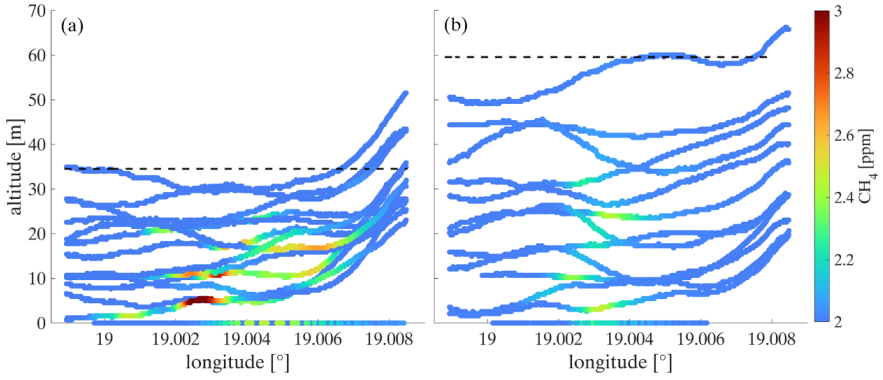

Figure 12. Cross section of CH_4 measurements from multiple helicopter and mobile ground-based transects (here altitude = 0 m) through the plume during **(a)** Release 1, 17 October 2022, 12:37–13:34 local time and **(b)** Release 2, 18 October 2022, 09:37–10:18 local time at the Bielsko-Biala airfield. The dashed lines indicate the estimated top of the plume.

The estimated release rates of these three approaches range from 14 kg h^{-1} to 22 kg h^{-1} with uncertainties of 13 % to 70 % (see Table S5 in Supplement S6) and hence, are in the order of magnitude of the released amount of ~21 kg h^{-1}. Although the flight pattern during this simple release experiment deviated from those applied during the probing of the coal mine ventilation shafts (varying altitude during plume crossing, top of plume below 60 m), we conclude that besides detecting low CH_4 enhancements, our helicopter-borne method is also capable of quantifying small emission rates of ~20 kg h^{-1}. As this simple release experiment was successful it provides validation of our method's ability to reliably quantify CH_4 emissions from point sources with small emission rates.

4 Summary & Conclusions

Compared to mass balance approaches performed by research aircraft to quantify CH_4 emissions, the *HELiPOD* offers an overall more flexibility. Flights can be conducted by a local helicopter company, facilitating easier implementation, especially in countries with limited access for foreign research aircraft. As an external sling load, it requires no aeronautical certification, allowing for uncomplicated modifications. The versatility of the helicopter enables plume probing as close as several hundred meters downwind, providing full vertical plume coverage from 50 m to 3 km altitude. This capability is particularly advantageous for probing, separating, and quantifying individual sources in complex emission landscapes. We showed that our helicopter-borne method can effectively quantify CH_4 emissions from coal mine ventilation shafts and drainage stations. These results are based on an explicit flight strategy.

An optimal sampling strategy strongly depends on local conditions such as emission source strength, meteorological factors (e.g., wind, atmospheric stability), the temporal resolution of deployed instruments, the velocity of the measurement platform, and the surrounding environment (e.g., vegetation, topography, remoteness). However, based on our experience, several lessons learned can be drawn to retrieve reliable mass flux estimates of CH_4 point sources using a helicopter-based approach:

- Constant wind conditions with speed of 3 m s^{-1} to 10 m s^{-1} and a consistent wind direction (RMSE < 30 °) reduce mass flux uncertainty.
- Ideally, full plume coverage from the bottom (as low as safe to fly, preferably below 100 m) to the plume top should be achieved, with vertical distances of 25 m to 100 m between transects.
- Assessment of the top of the plume before and after every point source probing through vertical profile measurements.

https://doi.org/10.5194/egusphere-2025-1010
Preprint. Discussion started: 12 March 2025

- Temporally tight probing of a MBE through the plume (less than 60 minutes per MBE) to ensure constant meteorological conditions.
- Sequential probing from the lowest to the highest altitudes or vice versa.
- Including mobile ground-based measurements, especially close to the emission source, reduces the uncertainty.
- Conducting ≥ 2 MBEs increases the statistical significance.
- Conducting one upwind curtain allows to assess the overall CH_4 background.

Additionally, a simple CH_4 release experiment was conducted. Results show that the helicopter-borne method can detect and quantify small emission rates down to 20 kg h^{-1} from single point sources. This emphasises the wide range of potential applications in quantifying sources with both lower CH_4 emissions, e.g. from biodigesters, landfills, cattle feedlots and manure pits, and higher emissions from industrial activities, making the *HELiPOD* an ideal tool to support reduction efforts of such emissions in the coal, O&G, agriculture and the waste sector.

Our confidence with the quality of the mass balance approach is reinforced by the close agreement with time synchronised quantifications derived from in-mine CH_4 safety sensor and air flow data. Our estimated top-down mean mass fluxes align with bottom-up in-mine data, all within the uncertainty range and without statistically significant bias. The variability that both approaches capture shows not only that reconciliation between these vastly different approaches was successful, but it reinforces the limitation of comparing short term (1-hour) campaign measurements with annual average emission inventory data. Our results support the application of the mass balance approach to define emission fluxes from industrial sources and the possibility of applying continuously derived in-mine data for greenhouse gas (GHG) reporting from coal mine ventilation shafts, emphasising the benefits of both approaches.

However, from the close agreement of both approaches one cannot conclude that more complex top-down measurements can generally be substituted by bottom-up data. This depends first on the emission landscape wherein the estimates are made and second on the quality of measurements. The coal mine ventilation shafts in Poland are strong and well-defined CH_4 point sources with good conditions to reliably estimate mass fluxes, which is the reason why we chose them to test our helicopter-borne approach. Regarding the quality of measurements, we note that the accuracy and representativeness of derived in-mine data depends on the applied technology and the applied location in the ventilation system and independent on-site measurements should evaluate their usability for GHG reports. In more complex environments like the oil and gas, the waste and the agriculture sector with their partly diffuse CH_4 emissions, bottom-up methods can only deliver rough estimates and top-down approaches are mandatory to quantify emissions more accurately.

The ability to separate co-located emission sources allowed us to study an additional shaft and three drainage stations which were located close to the targeted shafts. We measured emissions of drainage stations for the first time independently and found that they can be of the same order of magnitude, as those from ventilation shafts. Hence drainage stations are not negligible CH_4 emission sources in Poland and should be reported on separately. But more measurements of drainage station emissions are necessary to verify these findings.

Our helicopter-borne mass balance approach has recently been deployed in a study on further anthropogenic sources from the oil, gas, and waste sectors on the Arabian Peninsula, which will be addressed in a separate publication. The approach closes the gap between ground-based measurements near the source and far-field airborne and satellite measurements, allowing us to separate and quantify emissions from nearby sources. It serves as an independent emission verification tool and will assist coal, oil, and gas companies, as well as governments, in prioritizing their CH_4 emission mitigation strategies, actions, and policies.

https://doi.org/10.5194/egusphere-2025-1010
Preprint. Discussion started: 12 March 2025

Data availability. Data is available upon request. *HELiPOD* measurements will be made available through a data base later on.

Supplement. Supplementary material is separately available.

Author contributions. The paper was written and the figures were prepared by EF with contributions from HH. The experimental design and flight planning were performed by HH, AR, FP and EF. *HELiPOD* supervision and data processing were performed by FP, LB, AS, SB and AL. Mobile ground-based measurements were conducted and processed by PJ and JN. The bottom-up industrial data were obtained by JS. Picarro and Licor calibrations were performed by ML and DP. The controlled release experiment was conducted by ML. All authors contributed to the discussion of the results and the improvement of the manuscript.

Competing interests. The authors declare that they have no conflict of interest.

Acknowledgements. We thank David Holl from the University Hamburg, Institute of Soil Science, Hamburg, Germany for the loan of the Licor LI-7700.
The industrial data were obtained with courtesy of the mine management company JSW S.A. and PGG S.A.
JN and PJ acknowledge the "Excellence Initiative: Research University" program at AGH University of Science and Technology for financing the use of equipment.

Financial support. This research has been funded in the framework of UNEP´s International Methane Emissions Observatory (IMEO).

References

Andersen, T., Vinkovic, K., de Vries, M., Kers, B., Necki, J., Swolkien, J., Roiger, A., Peters, W., and Chen, H.: Quantifying methane emissions from coal mining ventilation shafts using an unmanned aerial vehicle (UAV)-based active AirCore system, Atmospheric Environment: X, 12, 100135, https://doi.org/10.1016/j.aeaoa.2021.100135, 2021.

Andersen, T., Zhao, Z., De Vries, M., Necki, J., Swolkien, J., Menoud, M., Röckmann, T., Roiger, A., Fix, A., Peters, W., and Chen, H.: Local-to-regional methane emissions from the Upper Silesian Coal Basin (USCB) quantified using UAV-based atmospheric measurements, Atmos. Chem. Phys., 23, 5191–5216, https://doi.org/10.5194/acp-23-5191-2023, 2023.

Burgués, J. and Marco, S.: Environmental chemical sensing using small drones: A review, Science of The Total Environment, 748, 141172, https://doi.org/10.1016/j.scitotenv.2020.141172, 2020.

Cambaliza, M. O. L., Shepson, P. B., Caulton, D. R., Stirm, B., Samarov, D., Gurney, K. R., Turnbull, J., Davis, K. J., Possolo, A., Karion, A., Sweeney, C., Moser, B., Hendricks, A., Lauvaux, T., Mays, K., Whetstone, J., Huang, J., Razlivanov, I., Miles, N. L., and Richardson, S. J.: Assessment of uncertainties of an aircraft-based mass balance approach for quantifying urban greenhouse gas emissions, Atmos. Chem. Phys., 14, 9029–9050, https://doi.org/10.5194/acp-14-9029-2014, 2014.

Chinas Ministry of Ecology and Environment: Methane Emissions Control Action Plan, Chinas Ministry of Ecology and Environment, 2023.

Chulakadabba, A., Sargent, M., Lauvaux, T., Benmergui, J. S., Franklin, J. E., Chan Miller, C., Wilzewski, J. S., Roche, S., Conway, E., Souri, A. H., Sun, K., Luo, B., Hawthrone, J., Samra, J., Daube, B. C., Liu, X., Chance, K., Li, Y., Gautam, R., Omara, M., Rutherford, J. S., Sherwin, E. D., Brandt, A., and Wofsy, S. C.: Methane point source quantification using MethaneAIR: a new airborne imaging spectrometer, Atmospheric Measurement Techniques, 16, 5771–5785, https://doi.org/10.5194/amt-16-5771-2023, 2023.

Conley, S., Faloona, I., Mehrotra, S., Suard, M., Lenschow, D. H., Sweeney, C., Herndon, S., Schwietzke, S., Pétron, G., Pifer, J., Kort, E. A., and Schnell, R.: Application of Gauss's theorem to quantify localized surface emissions from airborne

https://doi.org/10.5194/egusphere-2025-1010
Preprint. Discussion started: 12 March 2025

measurements of wind and trace gases, Atmospheric Measurement Techniques, 10, 3345–3358, https://doi.org/10.5194/amt-10-3345-2017, 2017.

Crosson, E. R.: A cavity ring-down analyzer for measuring atmospheric levels of methane, carbon dioxide, and water vapor, Appl. Phys. B, 92, 403–408, https://doi.org/10.1007/s00340-008-3135-y, 2008.

Dreger, M. and Kędzior, S.: Methane emissions against the background of natural and mining conditions in the Budryk and Pniówek mines in the Upper Silesian Coal Basin (Poland), Environ Earth Sci, 80, 746, https://doi.org/10.1007/s12665-021-10063-4, 2021.

Fiehn, A., Kostinek, J., Eckl, M., Klausner, T., Gałkowski, M., Chen, J., Gerbig, C., Röckmann, T., Maazallahi, H., Schmidt, M., Korbeń, P., Nęcki, J., Jagoda, P., Wildmann, N., Mallaun, C., Bun, R., Nickl, A.-L., Jöckel, P., Fix, A., and Roiger, A.: Estimating CH_4, CO_2 and CO emissions from coal mining and industrial activities in the Upper Silesian Coal Basin using an aircraft-based mass balance approach, Atmospheric Chemistry and Physics, 20, 12675–12695, https://doi.org/10.5194/acp-20-12675-2020, 2020.

Förster, E., Huntrieser, H., Maier, N., Pätzold, F., Bretschneider, L., Lampert, A., Nęcki, J., Jagoda, P., Bartyzel, J., and Roiger, A.: First airborne CH4 measurements on the Arabian Peninsula and estimation of CH4 mass fluxes from emissions of the oil, gas and waste sector., in preparation for ACP.

Forster, P., Storelvmo, T., Armour, K., Collins, W., Dufresne, J.-L., Frame, D., Lunt, D. J., Mauritsen, T., Palmer, M. D., Watanabe, M., Wild, M., and Zhang, H.: The Earth's Energy Budget, Climate Feedbacks, and Climate Sensitivity. In Climate Change 2021: The Physical Science Basis. Contribution of Working Group I to the Sixth Assessment Report of the Intergovernmental Panel on Climate Change, 1st ed., Cambridge University Press, https://doi.org/10.1017/9781009157896, 2021.

Foulds, A., Allen, G., Shaw, J. T., Bateson, P., Barker, P. A., Huang, L., Pitt, J. R., Lee, J. D., Wilde, S. E., Dominutti, P., Purvis, R. M., Lowry, D., France, J. L., Fisher, R. E., Fiehn, A., Pühl, M., Bauguitte, S. J. B., Conley, S. A., Smith, M. L., Lachlan-Cope, T., Pisso, I., and Schwietzke, S.: Quantification and assessment of methane emissions from offshore oil and gas facilities on the Norwegian continental shelf, Atmospheric Chemistry and Physics, 22, 4303–4322, https://doi.org/10.5194/acp-22-4303-2022, 2022.

France, J. L., Bateson, P., Dominutti, P., Allen, G., Andrews, S., Bauguitte, S., Coleman, M., Lachlan-Cope, T., Fisher, R. E., Huang, L., Jones, A. E., Lee, J., Lowry, D., Pitt, J., Purvis, R., Pyle, J., Shaw, J., Warwick, N., Weiss, A., Wilde, S., Witherstone, J., and Young, S.: Facility level measurement of offshore oil and gas installations from a medium-sized airborne platform: method development for quantification and source identification of methane emissions, Atmospheric Measurement Techniques, 14, 71–88, https://doi.org/10.5194/amt-14-71-2021, 2021.

Geiger, R., Aron, R. H., and Todhunter, P.: The Climate Near the Ground, Vieweg+Teubner Verlag, Wiesbaden, https://doi.org/10.1007/978-3-322-86582-3, 1995.

Gorchov Negron, A. M., Kort, E. A., Conley, S. A., and Smith, M. L.: Airborne Assessment of Methane Emissions from Offshore Platforms in the U.S. Gulf of Mexico, Environ. Sci. Technol., 54, 5112–5120, https://doi.org/10.1021/acs.est.0c00179, 2020.

Granier, C., Darras, S., Denier van der Gon, H., Doubalova, J., Elguindi, N., Galle, B., Gauss, M., Guevara, M., Jalkanen, J.-P., Kuenen, J., Liousse, C., Quack, B., Simpson, D., and Sindelarova, K.: The Copernicus Atmosphere Monitoring Service global and regional emissions (April 2019 version), https://doi.org/10.24380/D0BN-KX16, 2019.

Hajny, K. D., Lyon, D. R., Armstrong, A., Floerchinger, C. R., Jayarathne, T., Kaeser, R., Lavoie, T., Salmon, O. E., Stirm, B. H., Stuff, A. A., Tomlin, J. M., Wulle, B., Lopez-Coto, I., and Shepson, P. B.: Assessing the bias and uncertainties in the aircraft mass balance technique for the determination of carbon dioxide emission rates, Elementa: Science of the Anthropocene, 11, 00135, https://doi.org/10.1525/elementa.2022.00135, 2023.

Harmsen, M., van Vuuren, D. P., Bodirsky, B. L., Chateau, J., Durand-Lasserve, O., Drouet, L., Fricko, O., Fujimori, S., Gernaat, D. E. H. J., Hanaoka, T., Hilaire, J., Keramidas, K., Luderer, G., Moura, M. C. P., Sano, F., Smith, S. J., and Wada, K.: The role of methane in future climate strategies: mitigation potentials and climate impacts, Climatic Change, 163, 1409–1425, https://doi.org/10.1007/s10584-019-02437-2, 2020.

Heimburger, A. M. F., Harvey, R. M., Shepson, P. B., Stirm, B. H., Gore, C., Turnbull, J., Cambaliza, M. O. L., Salmon, O. E., Kerlo, A.-E. M., Lavoie, T. N., Davis, K. J., Lauvaux, T., Karion, A., Sweeney, C., Brewer, W. A., Hardesty, R. M., and Gurney, K. R.: Assessing the optimized precision of the aircraft mass balance method for measurement of urban greenhouse gas emission rates through averaging, Elementa: Science of the Anthropocene, 5, 26, https://doi.org/10.1525/elementa.134, 2017.

https://doi.org/10.5194/egusphere-2025-1010
Preprint. Discussion started: 12 March 2025

Höglund-Isaksson, L.: Global anthropogenic methane emissions 2005–2030: technical mitigation potentials and costs, Atmospheric Chemistry and Physics, 12, 9079–9096, https://doi.org/10.5194/acp-12-9079-2012, 2012.

Höglund-Isaksson, L.: Bottom-up simulations of methane and ethane emissions from global oil and gas systems 1980 to 2012, Environ. Res. Lett., 12, 024007, https://doi.org/10.1088/1748-9326/aa583e, 2017.

Höglund-Isaksson, L., Gómez-Sanabria, A., Klimont, Z., Rafaj, P., and Schöpp, W.: Technical potentials and costs for reducing global anthropogenic methane emissions in the 2050 timeframe –results from the GAINS model, Environ. Res. Commun., 2, 025004, https://doi.org/10.1088/2515-7620/ab7457, 2020.

Hsu, H. and Lachenbruch, P. A.: Paired T Test, in: Wiley StatsRef: Statistics Reference Online, edited by: Kenett, R. S., Longford, N. T., Piegorsch, W. W., and Ruggeri, F., Wiley, https://doi.org/10.1002/9781118445112.stat05929, 2014.

Huntrieser, H., Lichtenstern, M., Förster, E., Pätzold, F., Bretschneider, L., Lampert, A., Necki, J., Jagoda, P., Holl, D., and Roiger, A.-E.: Methane emissions from industrial activities: A novel airborne concept applied to coal mines in Poland also applicable for quantifying methane emissions from the oil & gas exploration and production in Oman?, International Conference on Air Pollution and Climate Change, Muscat, Oman, 2023a.

Huntrieser, H., Förster, E., Lichtenstern, M., Pätzold, F., Bretschneider, L., Lampert, A., Necki, J., Jagoda, P., Taupin, Q., Holl, D., and Roiger, A.: Quantifying methane emissions from industrial activities: A novel helicopter-borne application for coal mine ventilation shafts in Poland and perspectives, EGU23, https://doi.org/10.5194/egusphere-egu23-9152, 2023b.

Jagoda, P., Nęcki, J., Bartyzel, J., and Swolkień, J.: Mobile measurements of coal mine ventilation shafts in USCB, Poland., 11832, https://doi.org/10.5194/egusphere-egu24-11832, 2024.

Journal of Laws: Regulation of the Minister of Energy on detailed requirements for operating underground mining plants, 23 November 2016, item 1118 (in Polish), Warsaw, 2017.

Karacan, C. Ö., Field, R. A., Olczak, M., Kasprzak, M., Ruiz, F. A., and Schwietzke, S.: Mitigating climate change by abating coal mine methane: A critical review of status and opportunities, International Journal of Coal Geology, 295, 104623, https://doi.org/10.1016/j.coal.2024.104623, 2024.

Kelly, B. F. J., Lu, X., Harris, S. J., Neininger, B. G., Hacker, J. M., Schwietzke, S., Fisher, R. E., France, J. L., Nisbet, E. G., Lowry, D., van der Veen, C., Menoud, M., and Röckmann, T.: Atmospheric methane isotopes identify inventory knowledge gaps in the Surat Basin, Australia, coal seam gas and agricultural regions, Atmospheric Chemistry and Physics, 22, 15527–15558, https://doi.org/10.5194/acp-22-15527-2022, 2022.

Kirschke, S., Bousquet, P., Ciais, P., Saunois, M., Canadell, J. G., Dlugokencky, E. J., Bergamaschi, P., Bergmann, D., Blake, D. R., Bruhwiler, L., Cameron-Smith, P., Castaldi, S., Chevallier, F., Feng, L., Fraser, A., Heimann, M., Hodson, E. L., Houweling, S., Josse, B., Fraser, P. J., Krummel, P. B., Lamarque, J.-F., Langenfelds, R. L., Le Quéré, C., Naik, V., O'Doherty, S., Palmer, P. I., Pison, I., Plummer, D., Poulter, B., Prinn, R. G., Rigby, M., Ringeval, B., Santini, M., Schmidt, M., Shindell, D. T., Simpson, I. J., Spahni, R., Steele, L. P., Strode, S. A., Sudo, K., Szopa, S., van der Werf, G. R., Voulgarakis, A., van Weele, M., Weiss, R. F., Williams, J. E., and Zeng, G.: Three decades of global methane sources and sinks, Nature Geosci, 6, 813–823, https://doi.org/10.1038/ngeo1955, 2013.

Korbeń, P., Jagoda, P., Maazallahi, H., Kammerer, J., Nęcki, J. M., Wietzel, J. B., Bartyzel, J., Radovici, A., Zavala-Araiza, D., Röckmann, T., and Schmidt, M.: Quantification of methane emission rate from oil and gas wells in Romania using ground-based measurement techniques, Elementa: Science of the Anthropocene, 10, 00070, https://doi.org/10.1525/elementa.2022.00070, 2022.

Kostinek, J., Roiger, A., Eckl, M., Fiehn, A., Luther, A., Wildmann, N., Klausner, T., Fix, A., Knote, C., Stohl, A., and Butz, A.: Estimating Upper Silesian coal mine methane emissions from airborne in situ observations and dispersion modeling, Atmospheric Chemistry and Physics, 21, 8791–8807, https://doi.org/10.5194/acp-21-8791-2021, 2021.

Krautwurst, S., Gerilowski, K., Borchardt, J., Wildmann, N., Gałkowski, M., Swolkień, J., Marshall, J., Fiehn, A., Roiger, A., Ruhtz, T., Gerbig, C., Necki, J., Burrows, J. P., Fix, A., and Bovensmann, H.: Quantification of CH_4 coal mining emissions in Upper Silesia by passive airborne remote sensing observations with the Methane Airborne MAPper (MAMAP) instrument during the CO_2 and Methane (CoMet) campaign, Atmospheric Chemistry and Physics, 21, 17345–17371, https://doi.org/10.5194/acp-21-17345-2021, 2021.

Leelőssy, Á., Molnár, F., Izsák, F., Havasi, Á., Lagzi, I., and Mészáros, R.: Dispersion modeling of air pollutants in the atmosphere: a review, Open Geosciences, 6, 257–278, https://doi.org/10.2478/s13533-012-0188-6, 2014.

https://doi.org/10.5194/egusphere-2025-1010
Preprint. Discussion started: 12 March 2025

Luther, A., Kleinschek, R., Scheidweiler, L., Defratyka, S., Stanisavljevic, M., Forstmaier, A., Dandocsi, A., Wolff, S., Dubravica, D., Wildmann, N., Kostinek, J., Jöckel, P., Nickl, A.-L., Klausner, T., Hase, F., Frey, M., Chen, J., Dietrich, F., Nęcki, J., Swolkień, J., Fix, A., Roiger, A., and Butz, A.: Quantifying CH_4 emissions from hard coal mines using mobile sun-viewing Fourier transform spectrometry, Atmospheric Measurement Techniques, 12, 5217–5230, https://doi.org/10.5194/amt-12-5217-2019, 2019.

Luther, A., Kostinek, J., Kleinschek, R., Defratyka, S., Stanisavljević, M., Forstmaier, A., Dandocsi, A., Scheidweiler, L., Dubravica, D., Wildmann, N., Hase, F., Frey, M. M., Chen, J., Dietrich, F., Nęcki, J., Swolkień, J., Knote, C., Vardag, S. N., Roiger, A., and Butz, A.: Observational constraints on methane emissions from Polish coal mines using a ground-based remote sensing network, Atmospheric Chemistry and Physics, 22, 5859–5876, https://doi.org/10.5194/acp-22-5859-2022, 2022.

McDermitt, D., Burba, G., Xu, L., Anderson, T., Komissarov, A., Riensche, B., Schedlbauer, J., Starr, G., Zona, D., Oechel, W., Oberbauer, S., and Hastings, S.: A new low-power, open-path instrument for measuring methane flux by eddy covariance, Appl. Phys. B, 102, 391–405, https://doi.org/10.1007/s00340-010-4307-0, 2011.

McLinden, C. A., Griffin, D., Davis, Z., Hempel, C., Smith, J., Sioris, C., Nassar, R., Moeini, O., Legault-Ouellet, E., and Malo, A.: An Independent Evaluation of GHGSat Methane Emissions: Performance Assessment, Journal of Geophysical Research: Atmospheres, 129, e2023JD039906, https://doi.org/10.1029/2023JD039906, 2024.

Morales, R., Ravelid, J., Vinkovic, K., Korbeń, P., Tuzson, B., Emmenegger, L., Chen, H., Schmidt, M., Humbel, S., and Brunner, D.: Controlled-release experiment to investigate uncertainties in UAV-based emission quantification for methane point sources, Atmospheric Measurement Techniques, 15, 2177–2198, https://doi.org/10.5194/amt-15-2177-2022, 2022.

Naus, S., Maasakkers, J. D., Gautam, R., Omara, M., Stikker, R., Veenstra, A. K., Nathan, B., Irakulis-Loitxate, I., Guanter, L., Pandey, S., Girard, M., Lorente, A., Borsdorff, T., and Aben, I.: Assessing the Relative Importance of Satellite-Detected Methane Superemitters in Quantifying Total Emissions for Oil and Gas Production Areas in Algeria, Environ. Sci. Technol., 57, 19545–19556, https://doi.org/10.1021/acs.est.3c04746, 2023.

Nęcki, J. M., Bartyzel, J., Jagoda, P., Swolkień, J., Szlązak, N., Marek, K., Butler, N., and Field, R. A.: Quantifying methane emissions from a coal mine ventilation shaft using a pellistor safety sensor and a TDLAS analyzer: A case study from Poland., Atmospheric Measurement Techniques, in prep. for AMT.

Neininger, B. G., Kelly, B. F. J., Hacker, J. M., Lu, X., and Schwietzke, S.: Coal seam gas industry methane emissions in the Surat Basin, Australia: comparing airborne measurements with inventories, Philosophical Transactions of the Royal Society A: Mathematical, Physical and Engineering Sciences, 379, 20200458, https://doi.org/10.1098/rsta.2020.0458, 2021.

Nisbet, E. G., Fisher, R. E., Lowry, D., France, J. L., Allen, G., Bakkaloglu, S., Broderick, T. J., Cain, M., Coleman, M., Fernandez, J., Forster, G., Griffiths, P. T., Iverach, C. P., Kelly, B. F. J., Manning, M. R., Nisbet-Jones, P. B. R., Pyle, J. A., Townsend-Small, A., al-Shalaan, A., Warwick, N., and Zazzeri, G.: Methane Mitigation: Methods to Reduce Emissions, on the Path to the Paris Agreement, Reviews of Geophysics, 58, e2019RG000675, https://doi.org/10.1029/2019RG000675, 2020.

Pätzold, F., Bretschneider, L., Nowak, S., Brandt, B., Schlerf, A., Asmussen, M. O., Bollmann, S., Bärfuss, K., Harm-Altstädter, B., Hecker, P., Wehner, B., van der Wall, B. G., Sachs, T., Huntrieser, H., Roiger, A., and Lampert, A.: HELiPOD—Revolution and evolution of a helicopter-borne measurement system for multidisciplinary research in demanding environments, Elementa: Science of the Anthropocene, 11, 00031, https://doi.org/10.1525/elementa.2023.00031, 2023.

Pühl, M., Roiger, A., Fiehn, A., Gorchov Negron, A. M., Kort, E. A., Schwietzke, S., Pisso, I., Foulds, A., Lee, J., France, J. L., Jones, A. E., Lowry, D., Fisher, R. E., Huang, L., Shaw, J., Bateson, P., Andrews, S., Young, S., Dominutti, P., Lachlan-Cope, T., Weiss, A., and Allen, G.: Aircraft-based mass balance estimate of methane emissions from offshore gas facilities in the southern North Sea, Atmospheric Chemistry and Physics, 24, 1005–1024, https://doi.org/10.5194/acp-24-1005-2024, 2024.

Re3data.Org: ECCAD - the GEIA database; editing status 2023-11-30; re3data.org - Registry of Research Data Repositories, https://doi.org/10.17616/R35324, 2023.

Riddick, S. N., Mbua, M., Santos, A., Hartzell, W., and Zimmerle, D. J.: Potential Underestimate in Reported Bottom-up Methane Emissions from Oil and Gas Operations in the Delaware Basin, Atmosphere, 15, 202, https://doi.org/10.3390/atmos15020202, 2024.

Saunois, M., Stavert, A. R., Poulter, B., Bousquet, P., Canadell, J. G., Jackson, R. B., Raymond, P. A., Dlugokencky, E. J., Houweling, S., Patra, P. K., Ciais, P., Arora, V. K., Bastviken, D., Bergamaschi, P., Blake, D. R., Brailsford, G., Bruhwiler, L., Carlson, K. M., Carrol, M., Castaldi, S., Chandra, N., Crevoisier, C., Crill, P. M., Covey, K., Curry, C. L., Etiope, G., Frankenberg, C., Gedney, N., Hegglin, M. I., Höglund-Isaksson, L., Hugelius, G., Ishizawa, M., Ito, A., Janssens-Maenhout, G., Jensen, K. M., Joos, F., Kleinen, T., Krummel, P. B., Langenfelds, R. L., Laruelle, G. G., Liu, L., Machida, T., Maksyutov, S., McDonald, K. C., McNorton, J., Miller, P. A., Melton, J. R., Morino, I., Müller, J., Murguia-Flores, F., Naik, V., Niwa, Y.,

https://doi.org/10.5194/egusphere-2025-1010
Preprint. Discussion started: 12 March 2025

Noce, S., O'Doherty, S., Parker, R. J., Peng, C., Peng, S., Peters, G. P., Prigent, C., Prinn, R., Ramonet, M., Regnier, P., Riley, W. J., Rosentreter, J. A., Segers, A., Simpson, I. J., Shi, H., Smith, S. J., Steele, L. P., Thornton, B. F., Tian, H., Tohjima, Y., Tubiello, F. N., Tsuruta, A., Viovy, N., Voulgarakis, A., Weber, T. S., van Weele, M., van der Werf, G. R., Weiss, R. F., Worthy, D., Wunch, D., Yin, Y., Yoshida, Y., Zhang, W., Zhang, Z., Zhao, Y., Zheng, B., Zhu, Q., Zhu, Q., and Zhuang, Q.: The Global Methane Budget 2000–2017, Earth System Science Data, 12, 1561–1623, https://doi.org/10.5194/essd-12-1561-2020, 2020.

Schneising, O., Buchwitz, M., Reuter, M., Bovensmann, H., Burrows, J. P., Borsdorff, T., Deutscher, N. M., Feist, D. G., Griffith, D. W. T., Hase, F., Hermans, C., Iraci, L. T., Kivi, R., Landgraf, J., Morino, I., Notholt, J., Petri, C., Pollard, D. F., Roche, S., Shiomi, K., Strong, K., Sussmann, R., Velazco, V. A., Warneke, T., and Wunch, D.: A scientific algorithm to simultaneously retrieve carbon monoxide and methane from TROPOMI onboard Sentinel-5 Precursor, Atmospheric Measurement Techniques, 12, 6771–6802, https://doi.org/10.5194/amt-12-6771-2019, 2019.

Schuit, B. J., Maasakkers, J. D., Bijl, P., Mahapatra, G., van den Berg, A.-W., Pandey, S., Lorente, A., Borsdorff, T., Houweling, S., Varon, D. J., McKeever, J., Jervis, D., Girard, M., Irakulis-Loitxate, I., Gorroño, J., Guanter, L., Cusworth, D. H., and Aben, I.: Automated detection and monitoring of methane super-emitters using satellite data, Atmospheric Chemistry and Physics, 23, 9071–9098, https://doi.org/10.5194/acp-23-9071-2023, 2023.

Shindell, D., Sadavarte, P., Aben, I., Bredariol, T. de O., Dreyfus, G., Höglund-Isaksson, L., Poulter, B., Saunois, M., Schmidt, G. A., Szopa, S., Rentz, K., Parsons, L., Qu, Z., Faluvegi, G., and Maasakkers, J. D.: The methane imperative, Front. Sci., 2, https://doi.org/10.3389/fsci.2024.1349770, 2024.

Soulie, A., Granier, C., Darras, S., Zilbermann, N., Doumbia, T., Guevara, M., Jalkanen, J.-P., Keita, S., Liousse, C., Crippa, M., Guizzardi, D., Hoesly, R., and Smith, S. J.: Global anthropogenic emissions (CAMS-GLOB-ANT) for the Copernicus Atmosphere Monitoring Service simulations of air quality forecasts and reanalyses, Earth System Science Data, 16, 2261–2279, https://doi.org/10.5194/essd-16-2261-2024, 2024.

Student: The Probable Error of a Mean, Biometrika, 6, 1, https://doi.org/10.2307/2331554, 1908.

Swolkień, J.: Utilizing of Methane from Polish Hard Coal Mines, JEPE, 9, https://doi.org/10.17265/1934-8975/2015.02.004, 2015.

Swolkień, J., Fix, A., and Gałkowski, M.: Factors influencing the temporal variability of atmospheric methane emissions from Upper Silesia coal mines: a case study from the CoMet mission, Atmospheric Chemistry and Physics, 22, 16031–16052, https://doi.org/10.5194/acp-22-16031-2022, 2022.

Sykes, R. I., Lewellen, W. S., and Parker, S. F.: A Gaussian Plume Model of Atmospheric Dispersion Based on Second-Order Closure, Journal of Applied Meteorology and Climatology, 25, 322–331, https://doi.org/10.1175/1520-0450(1986)025<0322:AGPMOA>2.0.CO;2, 1986.

Tettenborn, J., Zavala-Araiza, D., Stroeken, D., Maazallahi, H., van der Veen, C., Hensen, A., Velzeboer, I., van den Bulk, P., Vogel, F., Gillespie, L., Ars, S., France, J., Lowry, D., Fisher, R., and Röckmann, T.: Improving Consistency in Methane Emission Quantification from the Natural Gas Distribution System across Measurement Devices, EGUsphere, 1–27, https://doi.org/10.5194/egusphere-2024-3620, 2025.

Thakur, P.: Chapter 8 - Coal Seam Degasification, in: Coal Bed Methane, edited by: Thakur, P., Schatzel, S., and Aminian, K., Elsevier, Oxford, 155–175, https://doi.org/10.1016/B978-0-12-800880-5.00008-5, 2014.

Tu, Q., Schneider, M., Hase, F., Khosrawi, F., Ertl, B., Necki, J., Dubravica, D., Diekmann, C. J., Blumenstock, T., and Fang, D.: Quantifying CH_4 emissions in hard coal mines from TROPOMI and IASI observations using the wind-assigned anomaly method, Atmospheric Chemistry and Physics, 22, 9747–9765, https://doi.org/10.5194/acp-22-9747-2022, 2022.

International Methane Emissions Observatory (IMEO): https://www.unep.org/topics/energy/methane/international-methane-emissions-observatory, last access: 16 February 2024.

UNEP: International Methane Emissions Observatory (IMEO) - Published & Ongoing Coordinated Scientific Studies on Methane, 2024.

Vaughn, T. L., Bell, C. S., Pickering, C. K., Schwietzke, S., Heath, G. A., Pétron, G., Zimmerle, D. J., Schnell, R. C., and Nummedal, D.: Temporal variability largely explains top-down/bottom-up difference in methane emission estimates from a natural gas production region, Proceedings of the National Academy of Sciences, 115, 11712–11717, https://doi.org/10.1073/pnas.1805687115, 2018.

https://doi.org/10.5194/egusphere-2025-1010
Preprint. Discussion started: 12 March 2025

WUG: Ocena stanu bezpieczeństwa pracy, ratownictwa górniczego oraz bezpieczeństwa powszechnego w związku z działalnością górniczo-geologiczną w 2022 roku, Wyższy Urząd Górniczy (State Mining Authority), 2023.